U.S. Department
of Transportation

**Federal Aviation
Administration**

ARP Fault Detection and Isolation: Method and Results

Project Memorandum
DOT-VNTSC-FA460-PM-93-21
December 1993

R. Grover Brown
Gerald Y. Chin
John H. Kraemer
Glau C. Nim
Karen L. Van Dyke

CENTER FOR NAVIGATION

Approved for Distribution:

M. J. Moroney

Division Chief

U.S. Department of Transportation
Research and Special Programs
Administration
Volpe National Transportation
Systems Center
Cambridge, MA 02142-1093

PREFACE

This study describes the development of a Receiver Autonomous Integrity Monitoring (RAIM) algorithm to meet the requirements for sole means navigation. The algorithm, referred to as a Fault Detection and Isolation (FDI) algorithm, is required not only to detect the presence of a faulty satellite in the navigation solution, but also to identify the faulty satellite and remove it from the solution.

The project memorandum describes the development of the algorithm, algorithm testing, and compares its performance to that of a somewhat similar Fault Detection and Exclusion (FDE) algorithm. The FDE algorithm operates with a set of six satellites and does not attempt to explicitly identify the faulty satellite, but merely to exclude it from the solution.

Results of an FDI availability study for CONUS are also given. These results are based upon GPS augmented with measurements from a barometric altimeter. Augmentations of GPS with geostationary and GLONASS satellites were also evaluated. FDI availability is given for the en route, terminal, and nonprecision approach phases of flight.

The work was performed in support of The Federal Aviation Administration. Ronald E. Morgan, Director, NAS Systems Engineering Service is the sponsor. David L. Olsen, ASE-310 is the sponsor's program manager and F. Charles Rosario, ASE-314 is the project engineer. The authors wish to thank their FAA sponsors for their support and encouragement.

TABLE OF CONTENTS

LIST OF FIGURES

LIST OF FIGURES (cont.)

LIST OF TABLES

1. INTRODUCTION

Since the development of the Wide Area GPS Augmentation (WGA) is not yet completed, integrity will be provided by the method known as Receiver Autonomous Integrity Monitoring (RAIM). The RAIM algorithm is contained within the aircraft equipment and makes use of redundant measurements to detect the presence of (and sometimes isolate) a faulty satellite. Also, RAIM may viewed as a backup integrity system when the WGA becomes operational.

RTCA Special Committee 159 (SC-159) has specified Minimum Operational Performance Standards (MOPS) for GPS as a supplementary navigation system [1]. Work is proceeding to specify the MOPS for GPS as a sole means navigation system.

This report documents the work done at the Volpe Center during fiscal year 1993. Section 2 provides background material and discusses the simulations performed. Section 3 provides a mathematical background for the Fault Detection and Isolation (FDI) algorithm which is the primary subject of this study. Section 4 discusses the operation of FDI including augmentation with a barometric altimeter. FDI availability results are presented in Section 5. Section 6 describes algorithm testing under dynamic conditions where ramp-type satellite failures are introduced. The ramp-type failure is intended to simulate a satellite clock frequency offset leading to a measurement error which increases linearly with time.

Preliminary results from a comparison of the FDI algorithm with the Fault Detection and Exclusion (FDE) algorithm are contained in Section 7. The FDE algorithm is currently being proposed as the baseline algorithm for the RTCA MOPS for sole means navigation using GPS. FDI availability results for CONUS are given in Section 8. Results are provided for GPS augmented with measurements from a barometric altimeter, as well as from geostationary and GLONASS satellites.

The table of integrity specifications as it appears in the RTCA supplemental MOPS [1] is reproduced in Table 1. These specifications are based upon worst case single-satellite failures. As used here, worst-case means that the error occurs in the satellite which is the most difficult to detect and that the satellite geometry is marginal for RAIM fault detection.

Requirements for the Alarm Limit, Time-to-Alarm and Minimum Detection Probability are expected to remain unchanged in the sole means MOPS. The Maximum Allowable Alarm Rate will be replaced by an availability specification.

Table 1 GPS Integrity Specifications

Phase of Flight	Performance Item			
	Alarm Limit	Maximum Allowable Alarm Rate	Time to Alarm	Minimum Detection Probability
En Route (Oceanic, Random, and J/V Routes)	2.0 nmi.	.002/hr.	30 sec.	.999
Terminal	1.0 nmi	.002/hr.	10 sec.	.999
Nonprecision Approach	0.3 nmi.	.002/hr.	10 sec.	.999

2. BACKGROUND

There are two approaches to implementing RAIM. One, which is called a "snapshot" scheme, uses only the current set of measurements. A second approach uses both current and past measurements and perhaps a priori information on aircraft dynamics. Such an approach might be referred to as an averaging scheme [2]. This study evaluates the "snapshot" approach.

Worst-case conditions are assumed in this study. This means that

(1) the failure (a bias error) is introduced into the most-difficult-to-detect satellite and

(2) the magnitude of the bias is chosen to maximize the missed detection probability.

Worst-case biases were recomputed from those used in earlier studies in order to accommodate the Optimized 24 Constellation.

Maximum admissible ARP values have been determined by Monte-Carlo simulation. ARP, the Approximate Radial-error Protected (ARP) Method, was developed by one of the authors (R.G. Brown) to determine the suitability of a given satellite geometry for RAIM [3-6]. It is used to screen out those geometries for which the FDI algorithm would not operate within the required specifications.

This study treats three phases of flight -- (a) nonprecision approach, (b) terminal, and (c) en route. Simulations are performed to determine the RAIM availability for:

(1) the initial stage of detection with the full set of n measurements and also for

(2) the second stage of the detection with a subset of (n-1) measurements after the isolation (removal) of one satellite, where n = the number of visible satellites plus a barometric altimeter (if included).

Simulations are performed both with and without barometric altimeter measurements.

The simulations are based upon the following:

- The test statistic chosen for this study is the square root of SSE (the sum of the squares of the measurement residuals). This is equivalent to choosing the norm of the parity vector $\mathbf{p}$ -- see M.A. Sturza and A.K. Brown [7,8]:

(1a) Test Statistic $= \|\mathbf{p}\| = \sqrt{(\mathbf{p}^T\mathbf{p})}$

(1b) $= \sqrt{(SSE)}$

- The Optimized 24 Constellation . The orbital elements for this constellation are

provided in Appendix A. This configuration is also known as the Optimized 21+3 or GPS Target Location Constellation.

- Mask angle = 7.5 deg.

- The 24 RTCA specified global locations [1] and 48 time points (a sample every half hour) spaced over 24 hours, beginning at the epoch: 1991, 12, 1, 0, 0, 0 (see Appendix A). The number of sampled space-time geometries is (24)(48) = 1152.

- The RTCA allowable conditional missed detection probability (Table 1) is 0.001.

- The alarm limits specified by RTCA are used in the current study. They are:

Nonprecision Approach Phase (NPA):	0.3 nmi	(555m);
Terminal Phase:	1.0 nmi	(1,852m);
En Route phase:	2.0 nmi	(3,704m).

- The standard deviation of the sum of the system noise and Selective Availability (SA) errors for the pseudorange measurement to each GPS satellite is assumed to be:

(2) $\sigma = 33.0$ m

- n measurements are available to the user equipment for a given geometry. The n measurements include the GPS satellites (and perhaps GLONASS and geostationary satellites) in view and, in some cases, a barometric altimeter measurement.

The test statistic used here is very similar to the one used by Parkinson and Axelrad [9-12]. The choice in this study differs from that used in earlier studies [4-6] by a factor of $\sqrt{(n-4)}$, where n is the number of measurements. Consequently, some of the formulae given below differ slightly from those used in earlier studies.

The RTCA supplemental navigation alarm rate is 1/15,000 alarms per sample when GPS is operating normally (no large bias or ramp in the measurements). This value is used here to calculate the detection (or decision) threshold for the test statistic.

A conditional missed detection probability of 0.001 was used in a previous study to obtain plots of the conditional miss rate vs. ARP for various geometries. These plots were then used to determine the ARP ceilings for different numbers of measurements and phases of flight. However, the satellite configuration used in the previous study was the Optimal 21 constellation. Those original ARP-ceilings have been revised in this study for use with the Optimized 24 Constellation.

3. INITIAL CALCULATIONS AND REVIEW

Before discussing the RAIM availability problem, some preliminary calculations are made and basic concepts are reviewed.

3.1 Calculating the Decision Threshold

Here one assumes that the system is working normally (no bias in the measurements) and the system noise and SA are such that there is a low probability of a false alarm. SSE (sum of the squares of the measurement residuals) has a chi-square distribution (unnormalized) with n-4 degrees of freedom, where n is the number of measurements [9,10,13].

For a given number of measurements, n, there is a corresponding chi-square density function given by the general formula [14]:

(3a) $$f_x(x;n) = \frac{x^{(n/2-1)}e^{-x/2}}{2^{n/2}\Gamma(n/2)}, \qquad \text{for } x > 0 \text{ and}$$

(3b) $$= 0, \qquad \text{for } x \le 0$$

where Γ is the gamma function. Some special density functions of interest are given in Appendix B.

The RTCA supplemental navigation false alarm requirement of 1/15,000 alarms per sample is used to set the decision threshold. The decision threshold "a" can be obtained from the following integral:

(4a) $$\int_0^a f_x(x;n)dx = 1 - \frac{1}{15,000}$$

or

(4b) $$\int_a^\infty f_x(x;n)dx = \frac{1}{15,000}$$

Given n, one can obtain the value of the decision threshold "a" assuming that the test statistic = SSE and $\sigma = 1.0$ m.

However, in this study the choice is that:

(5a) test statistic = $\sqrt{(SSE)}$ and

(5b) $$\sigma = 33.0\text{m}$$

Consequently, for this study

(5c) $\text{Threshold} = \sqrt{(a)(33.0)^2}$

3.1.1 Six-in-view Threshold Example

The following example is similar to that given previously by R.G. Brown [15]; the final threshold expression is different.

With n = 6, the number of degrees of freedom is 6 - 4 = 2. The corresponding chi-square probability density function for SSE is:

$$f_x(x) = \frac{1}{2} e^{-\frac{x}{2}}, \quad x \geq 0$$

The alarm rate is set at 1/15,000. The decision threshold is given by the upper limit of the integral of f_x such that

$$\int_0^n f_x(x)dx = 1 - \frac{1}{15,000}$$

In this case, the integral can be evaluated in closed form, and the solution is:

$$a = 2\ln(15,000) = 19.2316$$

This is the threshold one would use if SSE were the test statistic and the noise had σ of unity. However, $\sqrt{SSE}$ is the test statistic, and the noise σ is 33 m. Thus, the threshold to be used for an alarm rate of 1/15,000 and a noise σ of 33 m is

$$\text{Threshold} = \sqrt{(19.2316)(33)^2} = 144.7176 \text{ meters}$$

Table 2 provides the revised detection thresholds.

Table 2 Approximate Thresholds for Test Statistic Equal to $\sqrt{(SSE)}$; Noise Standard Deviation = 33 m; Alarm Rate = 1/15,000 (alarms per sample).

Number of Measurements (n)	Chi-Squared Degrees of Freedom	Detection Threshold (m)
5	1	131.599
6	2	144.718
7	3	154.608
8	4	162.980
9	5	170.366
10	6	177.066
11	7	183.248
12	8	189.021

3.2 Review of Basic Concepts and Formulae

3.2.1 Discussion

The following review is based on material given in previous studies [2-5]. The reader familiar with the previous studies may want to scan this material and go ahead to Section 4. Note that the symbol used to denote the projection matrix has been changed to **B**. The following terms are used in this study:

- ARP-ceiling: The largest admissible value of ARP for the given phase of flight and number of measurements, n.

- b: The magnitude of the bias in a given satellite pseudorange measurement.

- ET diagram: A diagram in which the test trajectory is plotted with the horizontal radial position error along the y-axis and the test statistic along the x-axis -- see Figure 2.

- FDE: Fault Detection and Exclusion.

- FDI: Fault Detection and Isolation.

- n: The number of measurements available in the initial stage of a FDI procedure.

- **I**: Identity or unit matrix.

- **G**: The linear connection matrix.

- **A**: This matrix transforms the range measurement error vector into the 4 by 1 navigation error response state vector, **x**.

(6) $\mathbf{A} \equiv (\mathbf{G}^T\mathbf{G})^{-1}\mathbf{G}^T$, (4 by n matrix).

- ε: The range measurement error vector.

(7) $\mathbf{x} = \mathbf{A}\varepsilon$

- **B**: The (n by n) projection or "hat" matrix.

(8) $\mathbf{B} \equiv \mathbf{G}(\mathbf{G}^T\mathbf{G})^{-1}\mathbf{G}^T$

- **w**: The range residual vector, which can be measured by the aircraft equipment.

- **p**: The parity vector.

The linear connection matrix **G** (a.k.a. data matrix) is obtained by linearizing the navigation equations about the nominal user position and clock bias-- **G** is known to the user. **G** has the dimension n by 4, where 4 is the dimension of the user state vector. The jth row of **G** can be expressed by $[-e_{j1}\ -e_{j2}\ -e_{j3}\ 1]$. The first three elements of the jth row are obtained by multiplying -1 by the direction cosines of the line of sight vector from the user to the jth satellite and the fourth element has the value of unity. By convention $-e_{jk}$ in **G** is often replaced by $+e_{jk}$. This is of no consequence.

The projection matrix **B** is denoted by **P** in some previous publications. The symbol **P** in this study denotes the parity matrix.

The parity vector **p** can be measured by the GPS receiver. It can be expressed as the product of the parity matrix **P** and the range measurement error vector ε. It can also be expressed as the product of the parity matrix and **y**, where **y** is the equivalent pseudorange measurement vector.

3.2.2 Deterministic or No-Noise Model

Some of the variables discussed below differ from the corresponding variables in previous publications by a factor $\sqrt{(n-4)}$. Since results from previous studies are used here, it is worthwhile to keep in mind those expressions which have changed and those which have remained the same. A detailed discussion is provided in Appendix C.

For a given user space-time geometry, one can calculate (theoretically) the deterministic (no-noise) parameters below.

Suppose that there are n satellites in view and let the bias, b, be on the jth satellite.

(9) $\underset{\text{(no-noise)}}{SSE(j,b)} = b^2 (1 - B_{jj})$,

where B_{jj} is the diagonal element on the jth row of the (n by n) projection matrix **B**:

(10a) $\underset{\text{(no-noise)}}{\text{Test Statistic}(j,b)} = \sqrt{SSE(j)}$

(10b) $= b\sqrt{(1-B_{jj})}$

The No-Noise Horizontal Radial Error is given by:

(11) $R_{hj}(b) = b\sqrt{(A_{1j}^2 + A_{2j}^2)}$

Now by definition for the no-noise case:

(12) SLOPE ≡ (Horiz. Nav. Radial Error) / (Test Statistic)

Substituting (10b) and (11) into (12) one obtains:

(13) $SLOPE(j) = \sqrt{\dfrac{(A_{1j}^2 + A_{2j}^2)}{(1-B_{jj})}}$

The user cannot measure the value of the bias. Notice that the bias b does not enter into the expression for SLOPE(j). However, it does matter on which satellite the bias occurs. For a given geometry, it is possible to compute a SLOPE for each satellite in view.

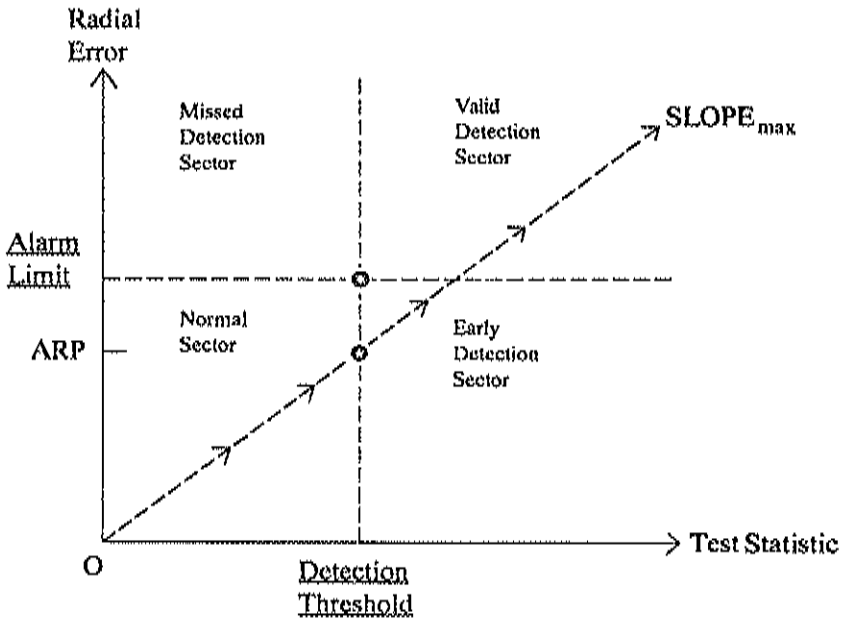

Figure 1 Deterministic Error Test Trajectory

The worst-case scenario occurs when the bias is on the "key" satellite-- corresponding to the satellite with the largest slope ($SLOPE_{max}$). The "key" satellite is the one associated with the "most-difficult-to-detect" failure. As a bias increases in time, the trajectory with $SLOPE_{max}$ passes closest to, or intrudes most deeply into, the missed detection sector. This is the sector where the trajectory enters the danger zone (the alarm limit is exceeded), but for an interval of time no warning flag is yet raised in the cockpit. When $SLOPE_{max}$ is very steep, this interval of time is long and the chance of a collision increases.

The trajectory with $SLOPE_{max}$ eventually intersects with the vertical dashed line of the detection or decision threshold. See Figure 1. The y-component of this intersection point is by definition the Approximate Radial-error Protected (ARP):

(14) $$\underset{\text{(meters)}}{ARP} = \underset{\text{(dimensionless)}}{SLOPE_{max}} \times \underset{\text{(meters)}}{\text{Detection Threshold}}$$

For any given space-time point, the following parameters are predictable and can be calculated ahead of time in flight planning or online by the aircraft's GPS receiver:

- n, the number of measurements (number of satellites in-view plus perhaps a barometric altimeter measurement;

- the value of SLOPE(j), if a bias error were to develop on the jth satellite;

- the "key" satellite (the one with the largest slope);

- the value of $SLOPE_{max}$ for the key satellite;
- the value of the detection threshold which is a function of n; and
- the value of ARP.

3.2.3 Stochastic Model

Here in the realistic stochastic model, the range measurement error includes system noise plus SA.

The sum of the squares of the measurement residuals is expressed by:

(15a) $SSE = \mathbf{w}^T\mathbf{w}$

(15b) $= \mathbf{y}^T(\mathbf{I} - \mathbf{B})\mathbf{y}$ (for measurements by the aircraft)

(15c) $= \boldsymbol{\varepsilon}^T(\mathbf{I} - \mathbf{B})^T(\mathbf{I} - \mathbf{B})\boldsymbol{\varepsilon}$

(15d) $= \boldsymbol{\varepsilon}^T(\mathbf{I} - \mathbf{B})\boldsymbol{\varepsilon}$

Eq. (15d) can be used in the simulation to obtain the values of SSE and the Test Statistic.

Note that the aircraft equipment cannot use equations (15c) or (15d) because the range measurement error vector, $\boldsymbol{\varepsilon}$, is not an observable quantity. The range residual vector, $\mathbf{y}$, is an observable quantity. When random noise is included, the test trajectory in the ET diagram traces in time an erratic path-- see Figure 2. The aircraft equipment can not calculate the y-axis component of this erratic trajectory, but can measure its x-axis component-- see Eq. (15b).

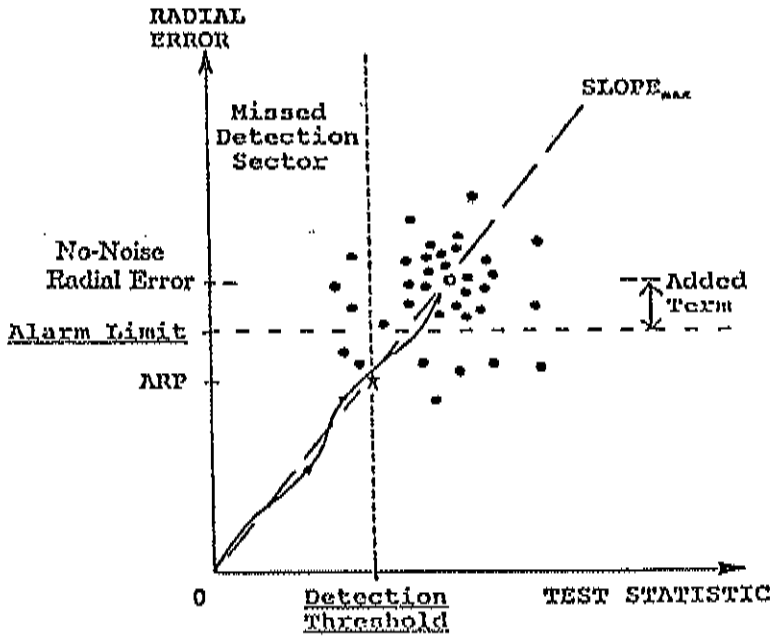

Figure 2 Term Added to the Alarm Limit, No-Noise Radial Error, and Cluster of Sample Points Intruding into Missed Detection Sector

If a bias were to be on the most-difficult-to-detect satellite, one could estimate the worst-case bias (or the equivalent parameter, the worst-case "Added Term") for each phase of flight. When the bias increases in time, the worst-case bias occurs when the number of missed detections is the largest. This depends on the phase of flight and on the number of measurements available (satellites plus barometric altimeter if available). Approximate values for the worst-case added terms are given in Table 3. Using the values from Table 3, one can estimate the ARP-ceiling values (revised recently for NPA) which are given in Table 4. Table 5 gives the ratio of ARP-ceiling to the alarm limit (revised).

Table 3 Ratio of Alarm Limit to Detection Threshold and Worst-Case Added Term

Phase of Flight	No. of Visible Satellites	Ratio y/x of Critical Point	Worst-Case Added Term (m)	Value Used (m)
NPA	6	555/102 = 5.44	-6.0	-6
Terminal	6	1852/102 = 18.16	14.9	15
En Route*	5	3704/132 = 28.06	58.8	62
En Route*	6	3704/102=36.31	65.1	

*Quadratic fits were used to obtain the worst-case Added Term for the en route case

Table 4 ARP-Ceiling Values for NPA, Terminal, and En Route Phases of Flight

Phase of Flight	Number of Satellites In-View				
	5	6	7	8	9 (or more)
Nonprecision Approach	327	338	349	359	361
Terminal	1074	1139	1139	1139	1139
En Route	2152	2269	2269	2269	2269

*The numbers in the 9 (or more) column are conservative estimated values. Very few nine-in-view geometries have ARP values this large.

TABLE 5 Ratio of ARP-Ceiling Values to Alarm Limit

Phase of Flight	Number of Satellites In-View				
	5	6	7	8	9 (or more)
Nonprecision Approach	.589	.608	.628	.646	.650
Terminal	.580	.615	.615	.615	.615
En Route	.581	.613	.613	.613	.613

4. RAIM COMPUTATION FOR DETECTION AND ISOLATION

This section provides a brief overview of the operation of the FDI algorithm and discusses inclusion of an input from a barometric altimeter. The computations are done using programs written in Turbo Pascal and MATLAB (*matrix laboratory*). MATLAB is an interactive software package for scientific and engineering numeric computation available from The MathWorks, Inc.

In the simulation, a MATLAB m-file is generated (this is an ASCII or text file) for each of the 1152 RTCA space-time points. Each m-file contains: the time, user latitude, and user longitude; n, the number of measurements in the initial set; and the n by 4 linear connection matrix **G**. (A Turbo Pascal program was developed that automatically generates the 1152 m-files.) The threshold values corresponding to various values of n (See Table 2) are stored in the main computer programs. MATLAB was used to perform the Monte Carlo simulations.

Figure 3 displays a flow chart for a Fault Detection and Isolation Algorithm (FDI). The algorithm has three stages. The first stage checks satellite geometry to determine if it is adequate for both the detection and isolation stages of FDI. The detection stage checks the internal consistency of the measurements as determined by the length of the parity vector. The third stage involves isolation of a faulty satellite following an initial detection. It should be pointed out that if a successful isolation is possible, there is no need to raise the alarm flag in the cockpit.

4.1 RAIM Availability for Fault Detection and Isolation (Sole Means Navigation)

This is a two stage operation -- see Figure 3. A necessary requirement is that the initial number of measurements be greater than or equal to 6. Two other test conditions based upon satellite geometry must also be met.

The first test determines if the geometry of the full set of n satellites is adequate to support the FDI algorithm. This test is given in condition (16). A second test, condition (17), is required to determine if each of the n subsets of (n-1) satellites is adequate to meet the detection requirement in the event that one satellite is removed (isolated) after an initial detection. The process is described in the following section.

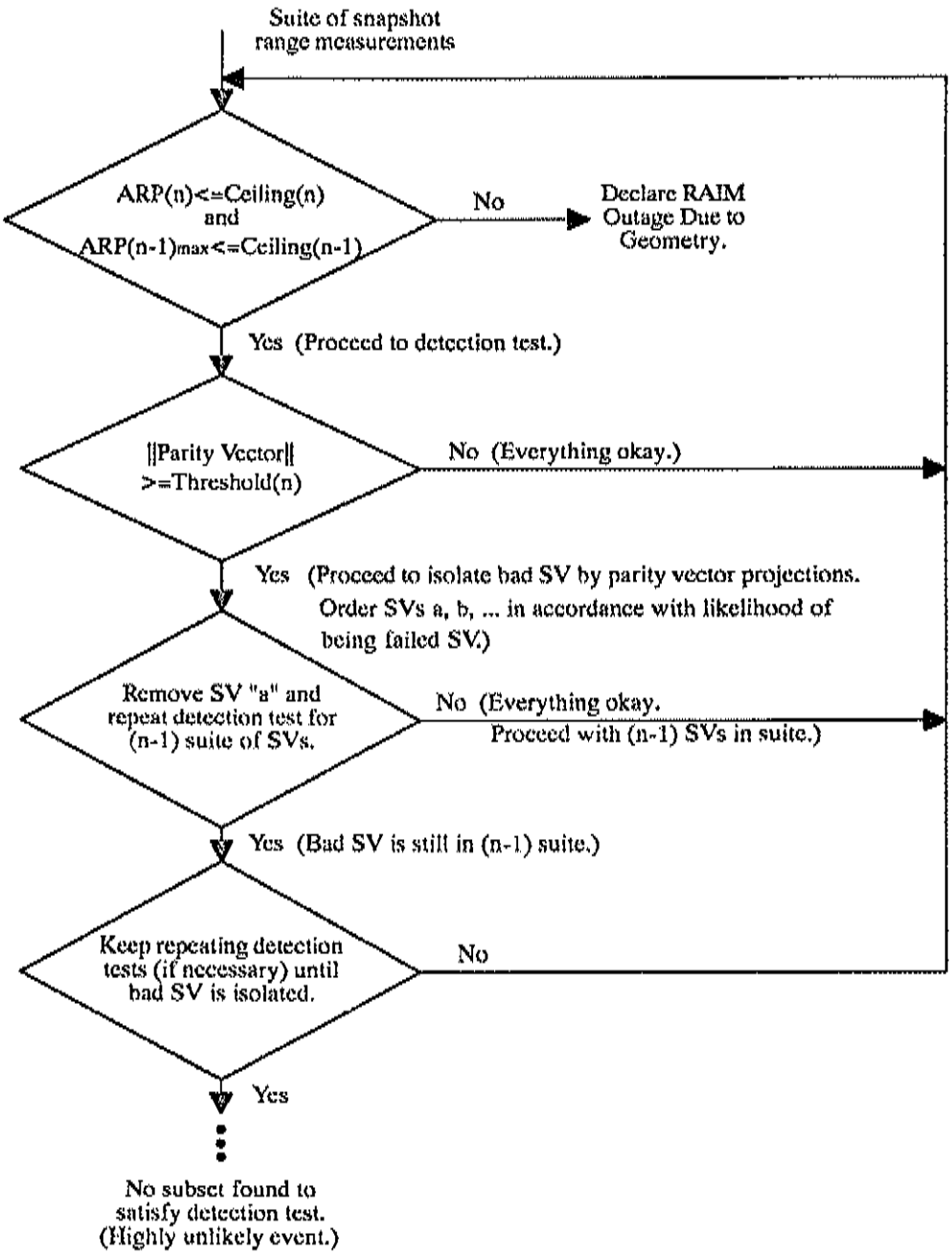

Figure 3 Flow Chart for FDI Algorithm

4.1.1 Case with No Barometric Altimeter Augmentation

For this case, where the barometric altimeter is not included, n measurements correspond to n visible GPS satellites.

The computer program determines the largest slope (see Section 3.2) and the ARP value. This is called ARPFULL and denotes the ARP for the full set of n measurements.

(16) $\quad ARPFULL \leq ARP\text{-}Ceiling(n)$

If condition (16) is false, RAIM is not available and a RAIM outage due to geometry is declared. If condition (16) is true, the satellite geometry is adequate for detection and the user satellite geometry must be evaluated for the isolation function.

There are n possible subsets of satellite, each containing (n-1) measurements. The computer program calculates the ARP for each of the subsets. The n ARP values are contained in a vector ARPSUB.

The worst-case situation must be evaluated. This is the case when the faulty (or omitted) satellite is such that the remaining subset of (n-1) measurements has the largest component in the ARPSUB vector. The program extracts this key component (denoted $ARPSUB_{max}$) and checks condition (17).

(17) $\quad ARPSUB_{max} \leq ARP\text{-}Ceiling(n\text{-}1)$

Since there are (n-1) measurements in the remaining subset, one uses the ARP-ceiling for the reduced set of measurements.

If this condition is true, the geometry is available for RAIM with Fault Detection and Isolation, otherwise the geometry is not available for FDI.

In summary, for RAIM FDI availability the following must be satisfied:

$\{ ARPFULL \leq ARP\text{-}Ceiling(n) \text{ and } ARPSUB_{max} \leq ARP\text{-}Ceiling(n\text{-}1)\}$

This completes the geometric stage of the FDI algorithm which screens out poor geometries. Note that it depends only on satellite geometry and does not involve pseudorange measurements. It is all that is needed to evaluate various satellite constellations for FDI coverage and availability. This is the criterion that is used in Section 8 which evaluates FDI availability for CONUS.

If the satellite geometry is adequate to support FDI, the measurements are next examined to determine their self consistency. This is the initial detection stage of the FDI algorithm. If the test statistic is below the detection threshold (See Table 2), operation is normal and the next set of measurements is examined.

If the test statistic exceeds the threshold for more than a given interval of time (discussed below), the isolation stage is initiated. This is called an internal alarm. No flag is raised in the cockpit at this point and the event is not uncommon.

In the case of the FDI algorithm, isolation is based upon the parity space method [7]. The method involves projecting the parity vector on each of n characteristic lines (one for each satellite or measurement) in parity space. See Figure 4. The satellites are rank ordered in accordance with the magnitude of the projections of the parity vector onto their characteristic lines. The satellite with the largest projection magnitude is considered to be the satellite most likely to be faulty.

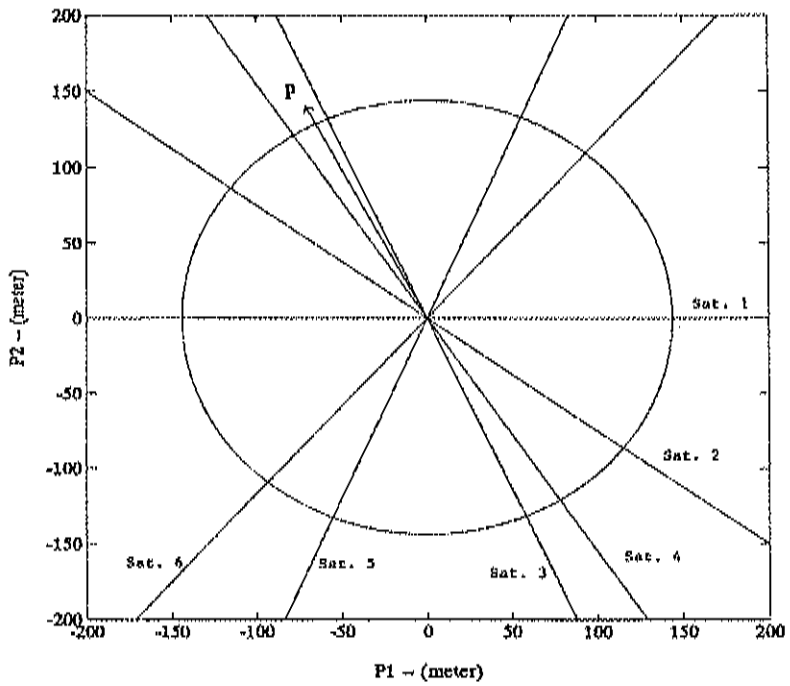

Figure 4 Parity Space Diagram for Six Satellites in View

The most likely satellite to have failed is removed from the set of n measurements. The detection test is repeated for the set of (n-1) measurements. If the ARP value falls below the new threshold (for n-1 measurements) and the test statistic is below the new (n-1) threshold, the faulty satellite is assumed to have been properly isolated. The algorithm returns to the usual detection stage and the next set of (n-1) measurements is examined. The algorithm is now working with a reduced set of measurements.

If, on the other hand, the test statistic exceeds the threshold, the faulty satellite is presumed to still be present in the set of n-1 measurements. The previously isolated satellite is returned to the measurement set and the next most likely candidate is removed. The test statistic is compared to the threshold and the process continues until the faulty satellite is isolated.

If no set of (n-1) measurements can be found with a test statistic that is below the threshold, a flag is raised in the cockpit notifying the pilot that RAIM is no longer available and GPS is believed to be out of tolerance. In the case of the simulation, where a two-second time step is used between measurements, the algorithm is given five attempts to isolate the faulty satellite before the flag is raised. This is based upon the requirement that the flag must be raised within ten seconds of violating the alarm limit for the nonprecision approach phase of flight. Longer time intervals might be used for other phases of flight.

4.1.2 Case with Inclusion of Barometric Altimeter Measurement

Here, a measurement from a barometric altimeter is added -- n denotes the sum of the measurements to the GPS satellites and the barometric measurement.

For the pseudorange measurement to each GPS satellite, one assumes that:

$$\sigma = 33.0 \text{ m}$$

The barometric altimeter measurement can be represented by an imaginary satellite located at the center of the earth. However, one must consider separately the standard deviations for the barometric altimeter measurement errors for different phases of flight. Appendix D gives more details on the rationale for obtaining the barometric altimeter σ-values. They are:

Nonprecision Approach: $\sigma_{baro} = 50$ m

Terminal Phase: $\sigma_{baro} = 300$ m

En route Phase: $\sigma_{baro} = 120$ m

For a given geometry, an extra row vector (whose values depends on the phase of flight) will be added to the "old" G-matrix for the GPS satellites to yield "new" G-matrix for the set of GPS satellites plus the imaginary (barometric altimeter) satellite. Details are given in Section 5.

5. SIMULATION PROCEDURE AND RESULTS FOR RTCA LOCATIONS

5.1 General Discussion

Several computer programs were developed for this study. This section provides a brief description of the simulation procedure and summarizes the results obtained.

Table 6 gives availability percentages for the 24 RTCA locations sampled at 30-minute intervals (1152 space-time points). Availability values are provided for both Fault Detection (supplemental use), as well as for Fault Detection and Isolation (sole means) navigation. Three phases of flight are included both with and without augmentation from a barometric altimeter.

Figure 5 shows the percentage of time that a given number of satellites are visible for the 1152 RTCA space-time points using the Optimized 24 Constellation and a 7.5 degree mask angle. When a barometric altimeter measurement is used, the number of measurements is increased by one. For example, Figure 5 shows that 6 measurements are available 11% of the time for GPS only. If a barometric altimeter measurement is included, then 7 measurements (6 satellites plus altimeter) are available 11% of the time.

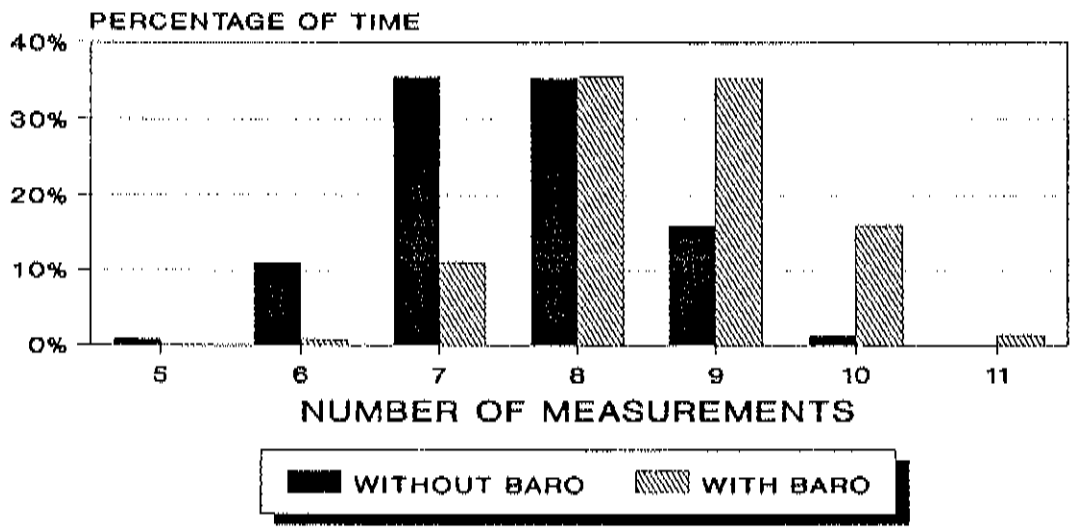

Figure 5 Satellite Visibility Distribution for 1152 RTCA Space-Time Points

The GPS-only (no altimeter) case is included for completeness and to show the sensitivity of RAIM to altimeter aiding. As noted in Section 8, unaided GPS is not a viable candidate for either supplemental or sole means navigation.

Detection-only results are important because full FDI capability is not always available following isolation of a faulty satellite. For example, isolation of a faulty satellite from a set of six satellites (no barometric altimeter) reduces the number of measurements to five. This limits the FDI algorithm to Fault Detection only.

The results given in Table 6 are based solely on satellite geometry and do not involve any Monte Carlo simulations.

Table 6 Availability Percentages for 24 RTCA Locations (1152 Space-Time Points, Optimized 24 Constellation, 7.5 degree Mask Angle)

CONFIGURATION	NPA	TERMINAL	EN ROUTE
Detection Only w/o Baro Aiding	95.4	99.4	99.8
Detection/Isolation w/o Baro Aiding	48.4	87.2	93.0
Detection Only with Baro Aiding	99.1	99.9	100.0
Detection/Isolation with Baro Aiding	78.9	94.3	99.1

Fault Detection and Isolation (FDI) Availability (no baro)

For a given geometry, the first stage of the program tests the RAIM availability for detection -- condition (16). If this condition is false, the space-time point is not available for RAIM.

If condition (16) is true, the point is counted as available for detection only. The program then goes to the second stage to test the condition for RAIM availability for detection after isolation, assuming a worst-case failure. The test is given by condition (17). A necessary requirement is that the initial or full number of measurements, n, be greater than or equal to 6. In what follows, only the geometries that have already passed condition (16) for the first stage are considered.

Nonprecision Approach:

(1) Consider the group of geometries with initial set of 6 measurements. The program counts the number of admissible geometries (RAIM available for detection and isolation) that have test result "true" for both condition (16) and condition (17). Condition (17) is in this instance given by:

$$ARPSUB_{max} \leq 327 \text{ m} \quad \text{(ARP-Ceiling(5))}$$

(The ARP-Ceilings are obtained from Table 4)

(2) Next, the group of geometries with initial or full set of 7 measurements is considered. The program counts the number of admissible geometries (RAIM available for FDI) that pass conditions (16) and (17). Here (17) is given by:

$$ARPSUB_{max} \leq 340.1 \text{ m} \quad \text{(ARP-Ceiling(6))}$$

(3) The program proceeds similarly for the cases of 8, 9, and 10 measurements.

(4) After summing the earlier results, one obtains:

NPA Availability = Total no. of admissible points / 1152

= 48.4 percent

This value is given in the second row, second column of data in Table 6. The terminal and the en route phases are examined in a similar manner. These results are given respectively in the third and fourth columns of Table 6.

Addition of Barometric Altimeter Measurement

For a given phase of flight, the relevant program sequentially examines each geometric file and adds a row to the original G-matrix for the addition of a barometric altimeter measurement.

The following G-matrices are used.

(A) Nonprecision Approach: The original G-matrix is modified to obtain

$$\mathbf{G} = \begin{bmatrix} (\text{Original} \\ \text{Satellite} \\ \text{G} - \text{Matrix}) \\ \cdots\cdots\cdots\cdots \\ 0 \quad 0 \quad .66 \quad 0 \end{bmatrix}$$

(B) Terminal Phase: The original G-matrix is modified to obtain

$$\mathbf{G} = \begin{bmatrix} (\text{Original} \\ \text{Satellite} \\ \text{G} - \text{Matrix}) \\ \cdots\cdots\cdots\cdots \\ 0 \quad 0 \quad .11 \quad 0 \end{bmatrix}$$

(C) En Route Phase: The original G-matrix is modified to obtain

$$\mathbf{G} = \begin{bmatrix} (\text{Original} \\ \text{Satellite} \\ \text{G} - \text{Matrix}) \\ \cdots\cdots\cdots\cdots\cdots \\ 0 \quad 0 \quad .275 \quad 0 \end{bmatrix}$$

The non-zero values in the last rows of the modified G-matrices are weighting factors (33 meters divided by σ_{baro}) to account for the differences between the pseudorange accuracy and the accuracy of the barometric altimeter measurement. FDI availability with barometric altimeter augmentation is computed as previously described.

The enhancement of availability due to augmentation from a barometric altimeter can be seen in Table 6. Detection-only availability exceeds 99% with the augmentation as opposed to 95.4% or better without augmentation. Full FDI availability improvement is more dramatic. Here, availability which ranges from 48.4% to 93.0% without augmentation increases to 78.9% to 99.1% with augmentation. Note that the values given in Table 6 relate only to the 24 RTCA locations. Much more extensive results for CONUS are given in Section 8 which includes additional augmentations.

6. DYNAMIC TESTS OF FDI ALGORITHM

This section treats the dynamic aspects of the FDI algorithm. The previous sections are mainly concerned with satellite geometry and its effect on FDI availability. This section deals with the algorithm's response to the growth of a pseudorange bias error. Error growth rates of 2 and 3 meters per second are evaluated. Worst-case satellite geometries are used in accordance with RTCA requirements. In particular, ten space-time points are selected for evaluation from the 1152 RTCA space-time points.

The 1152 space-time points are rank-ordered according to their ARP values for FDI. The selected points are those whose ARP values fall just below the ARP ceiling for the phase of flight in question. Only the Nonprecision Approach phase is considered in this section.

The Optimized 24 satellite constellation (see Appendix A) is used in the dynamic simulations. The pseudorange error contains a ramp of constant slope (2 or 3 meters per second) starting at the origin (t=0) and lasting for the ten-minute duration of the run.

The RTCA noise model is used to simulate Selective Availability errors. This model consists of a second-order Gauss-Markov process added to a random bias (held constant for the ten-minute duration of the run) and a white noise process intended to simulate receiver noise. The characteristics of the Gauss-Markov portion of the RTCA noise model are given in [16]. The autocorrelation function $R(\tau)$ of the pseudorange portion (2nd-order G-M) of the noise is given by [17] as

$$R_x(\tau) = \sigma^2 e^{-\alpha\tau} [\cos(\alpha\tau) + \sin(\alpha\tau)], \qquad \tau \geq 0$$

where $\omega_0 = 0.012$ rad/sec and $\alpha = \omega_0/\sqrt{2}$.

6.1 SA-induced Alarm Tests With Scaled-up Noise

The purpose of these tests is to test the SA-induced alarm rate using scaled-up noise in a manner similar to that proposed in the testing portion of the RTCA sole means MOPS.

If noise scaling proved feasible, it would greatly reduce the number of Monte-Carlo simulation runs required to assess the algorithm's performance, both with respect to miss rate with a satellite failure present and the false-alarm rate with no satellite failure.

Three marginal seven-in-view geometries (RTCA29, RTCA1019, and RTCA391) without barometric altimeter augmentation were selected for the alarm rate tests. The designations RTCA29, RTCA1019, and RTCA391 are included here only for the sake of completeness and traceability and have no meaning outside of the Volpe Center. Forty computer runs were made with each geometry (space-time point) with 301 independent samples per run. This gave (40)(301) = 12040 independent samples for each geometry. Each run was repeated three times with a different seed for the random number generator. The alarm rate was averaged over the

three runs for each of three geometries.

On the first attempt at noise scaling, the usual RTCA noise model was used. The RTCA model consists of three components: 1) a random bias with σ = 23 meters, 2) a second-order Gauss-Markov process with σ = 23 meters as described in [16] and a sampling interval of 120 seconds and 3) a receiver noise model (zero-mean Gaussian) with σ = 5.57 meters, giving a total noise RSS error of 33 meters. The noise variates for each run were scaled up by a factor of 1.5661 to give an anticipated alarm rate of 0.03. This scale factor is based upon an assumed statistical independence (zero correlation) among the samples.

The first noise scaling test yielded an alarm rate of 0.017 rather than the anticipated value of 0.03. This large difference, almost a factor of two, could not be explained as a statistical anomaly because of the large number of samples (12,040) used in the experiment.

It was recognized from the beginning, that the two-minute sampling interval would not yield truly independent samples when the RTCA noise model was used. To see if this was the source of the discrepancy observed in the first experiment (i.e. 0.017 experimental vs. 0.030 calculated false alarm rate), the experiment was re-run with the noise model changed to assure statistically independent samples.

In the second attempt, the random bias was removed and the Gauss-Markov process σ = 23 meters scaled up by a factor of $\sqrt{2}$. The sampling interval was changed from 120 seconds to 277.68 seconds. This sampling interval corresponds to the first zero-crossing of the autocorrelation function of the RTCA Gauss-Markov process. See Figure 6. This assured statistical independence among the samples. The results are shown in Table 7.

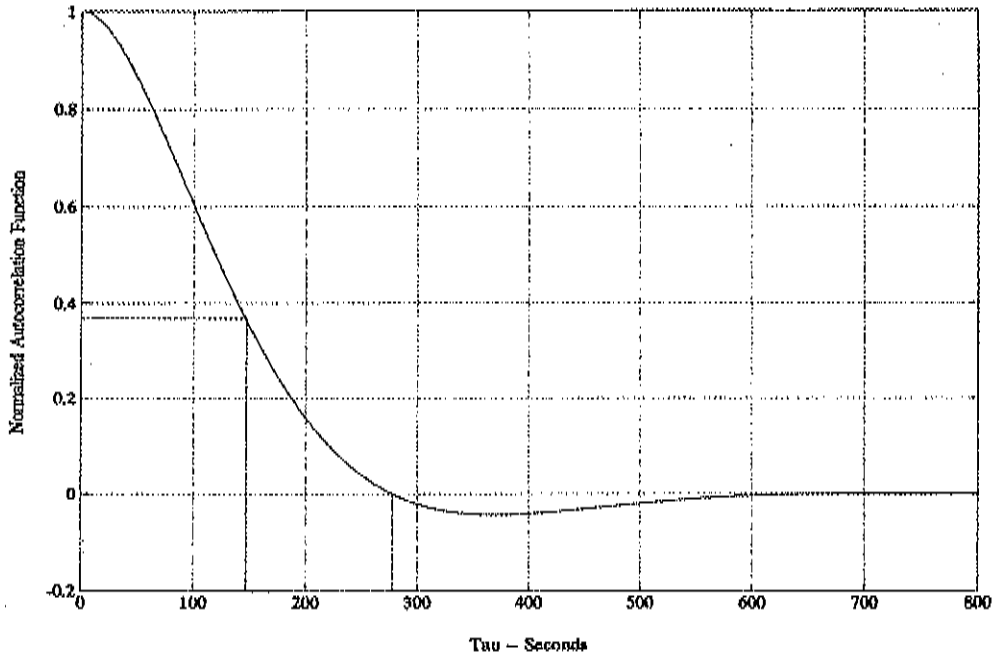

Figure 6 Autocorrelation Function for RTCA Gauss-Markov Process

Table 7 Scaled Alarm Rates for Seven-in-View Geometries (RTCA29, RTCA1019, and RTCA391)

RTCA29

Number of Samples	Number of Alarms	Alarm Rate	Starting Seed
12040	385	0.0320	1
12040	337	0.0280	201
12040	342	0.0284	3001
		Avg. 0.0295	

RTCA1019

Number of Samples	Number of Alarms	Alarm Rate	Starting Seed
12040	352	0.0292	1
12040	330	0.0274	201
12040	3889	0.0323	3001
		Avg. 0.0296	

RTCA391

Number of Samples	Number of Alarms	Alarm Rate	Starting Seed
12040	359	0.0298	1
12040	336	0.0279	201
12040	314	0.0261	3001
		Avg. 0.0279	

The alarm rate averaged over all of the runs is 0.0290 which is very close to the theoretical rate of 0.030. This shows that the problem is associated with the correlation among the samples and was not due to an error in the mathematics. Since it is not clear how to account for correlation among the samples, noise scaling is not used in this study. The test does show that noise scaling can be done in cases involving statistically independent samples and may be useful in bench-testing of user equipment.

6.2 Fault Detection and Isolation Tests (FDI Algorithm)

The purpose of these runs is to test the dynamic performance of the FDI algorithm.

The errors used in the simulation are generated as follows using a two-second sampling interval:

(1) Ramp of 2 meters/second placed into the most difficult to detect satellite.

(2) 2nd-order Gauss-Markov process (RTCA noise model) with $\sigma = 23$ meters.

(3) Random bias (constant for run) with $\sigma = 23$ meters.

(4) White Gaussian receiver noise with $\sigma = 5.57$ meters.

These noise components have an RSS value of 33 meters. One thousand ten-minute computer runs were made for each of ten marginal RTCA geometries. Three of the geometries had seven satellites in view, five geometries had eight satellites in view and two had nine satellites in view. The alarm limit was set to the NPA value of 555.6 meters (0.3 nmi.). A run was counted as a miss if, at any time during the ten-minute simulation, the horizontal navigation error exceeded the alarm limit for more than ten seconds before the detection threshold was exceeded.

The Monte Carlo simulation produced a total of 14 misses out of 10,000 ten-minute runs. This is reasonably close to the anticipated miss rate of 0.001. There were 8,785 correct isolations at the first detection, giving a correct isolation rate of nearly 90% at first detection.

6.2.1 SA-Induced Alarms

Some of the alarms in the dynamic tests were induced by SA. In those computer runs, the FDI algorithm successfully isolated the faulty satellite. At a later time, however, the alarm was triggered again by SA and the algorithm was unable to find a suitable subset of satellites with a

test statistic below the threshold. This is called an unresolved alarm. The purpose of the tests discussed in this section is to determine how the FDI algorithm performs in the presence of SA with **no ramp bias error** present.

50,000 trials were performed for each of ten geometries and the number of alarms was counted. The noise had an RSS value of 33 meters and no ramp error was present. A total of 43 SA-induced alarms were counted and the random number generator seeds recorded. These 43 cases were re-run to determine the number of subsets available with test statistics less than the threshold. This gives the number of available geometries the FDI algorithm can choose from in recovering from an SA-induced alarm. The number of available geometries ranged from two to seven and the algorithm was able to recover from all 43 SA-induced alarms. The conclusion is that the unresolved alarm phenomenon is not a significant problem when a satellite is operating normally (no bias error).

7. COMPARISON OF FDI AND FDE ALGORITHMS

The objective of the tests described in this section is to compare the performance of the FDI and FDE algorithms. Two sets of tests were run. The first set used alarm limits set equal to the protection radius given by the FDE algorithm. This was done because the satellite geometries were marginal geometries for NPA as determined by the FDI ARP threshold. The second set of tests used these same geometries, but with the NPA alarm limit of 555.6 meters. The satellite geometries were seven-satellite in-view geometries designated RTCA29, RTCA1019 and RTCA391. These are the same geometries discussed in Section 6.1. Additional testing is currently being performed with eight- and nine-satellite in-view geometries.

7.1 Seven-Satellite In-View Tests Using FDE Protection Radius

The following test parameters were used:

- 1000 Monte-Carlo simulations for each of three seven-satellite geometries.
- Ten-minute simulated real-time run duration. Sampling interval = 2 seconds. Total number of samples per run = 301.
- Ramp of 3 meters/second alternatively put into the two most difficult to isolate satellites. This gives a total of 6000 runs.
- Model for random errors: 1) Second-order Gauss-Markov process with $\sigma = 23$ meters., 2) random bias (constant for run) with $\sigma = 23$ meters, 3) white Gaussian receiver noise with $\sigma = 5.57$ meters. Total RSS error = 33 meters.
- Detection thresholds set to yield "internal" false alarm rate of 1/15,000 per sample for both algorithms.
- The alarm limit for the FDI algorithm is set equal to the maximum protection radius of the FDE algorithm.
- An unresolved alarm is declared when the algorithm can't find any subset of satellites with a test statistic less than the threshold. Both algorithms are allowed five successive tests before declaring an unresolved alarm. This is within the ten-second time-to-alarm for NPA since the algorithms are working at a two-second time step.

The performance of the two algorithms is very similar for the seven-satellite geometries. There were a total of 4 misses for the FDI algorithm and 3 misses for the FDE algorithm out of a total of 6,000 ten-minute runs for each algorithm. Thus, both algorithms did better than the 0.001 miss rate required by RTCA. The FDE algorithm results are consistent with the theory that an algorithm which sets the alarm limit at the calculated protection radius (Brenner method) should yield conservative results with respect to the miss rate.

The FDI algorithm made 4,948 correct isolations on first detection (82.5%) while the FDE algorithm had 4599 correct isolations on first detection (76.7%). Note that while the FDE algorithm does not attempt to identify the faulty satellite, there is very little difference between isolation and exclusion when working with seven-satellite geometries. This is because there is only one satellite in the excluded set. Neither algorithm encountered any unresolved alarms.

7.2 Seven-Satellite In-View Tests Using RTCA NPA Protection Radius

These tests use the same test parameters as given above in Section 7.1, except that the alarm limit was set to 555.6 meters (0.3 nautical miles) which is the Area Navigation (RNAV) nonprecision approach (NPA) requirement.

It should be noted that in these tests, the FDE algorithm is being treated somewhat unfairly since all three geometries would normally be rejected by the FDE algorithm. This is because the FDE protection radii fall between 577.1 meters (RTCA329) and 579.8 meters (RTCA29) which is nearly 25 meters above the NPA requirement of 555.6 meters. It does, however, provide information on the sensitivity of the algorithms to changes in the alarm limit when all other parameters are held constant.

Again, the performance of the two algorithms is very similar for seven-satellite geometries. There were a total of 8 misses for the FDI algorithm and 5 misses for the FDE algorithm. The FDI algorithm did slightly poorer and the FDE algorithm slightly better than the 0.001 miss rate (6 misses) required by RTCA.

The FDI algorithm made 4,948 correct isolations on first detection (82.5%) while the FDE algorithm made 4599 correct isolations on first detection (76.7%). These are the same values as are given in Section 7.1. The reason they remain unchanged is that the same detection thresholds are used in each case. The miss rates will change since different alarm limits are used in Sections 7.1 and 7.2. Neither algorithm encountered any unresolved alarms.

Although these tests involved several thousand runs, the number of error events (misses) was relatively small (fewer than ten). One should therefore expect a fair amount of scatter in the data and not assign any great significance to a difference of two or three misses either way. For example, if the probability of a miss is 0.001, the most likely number of misses in 6,000 statistically independent tries is 6. The probability of exactly k misses in n trials is given by the binomial distribution.

The binomial law is given by:

$$P\{x = k\} = \frac{n!}{k!(n-k)!} p^k (1-p)^{n-k}$$

The values for n = 6,000 and a miss probability of 0.001 are given in Table 8. Note that the

probabilities for exactly 5 or 6 misses differ only in the fourth decimal place. The maximum spread among the values for k ranging from 4 to 7 is only 17% (0.16070 - 0.13385)/0.16070.

Table 8 Probability of Exactly k Misses in 6,000 Trials for Miss Probability = 0.001 for Each Trial

k	PROBABILITY
1	0.01484
2	0.04457
3	0.08919
4	0.13385
5	0.16068
6	0.16070
7	0.13775
8	0.10329
9	0.06884
10	0.04128

8. FDI AVAILABILITY FOR CONUS

In this section, FDI availability over the entire CONUS is examined. This analysis expands on that presented in Section 5 for the 24 RTCA locations. More space/time points are evaluated and augmentations such as GLONASS and geostationary satellites are also considered.

8.1 Analysis Parameters for FDI Availability Study

8.1.1 GPS Constellation

The GPS target location constellation was used for this analysis. This constellation, also known as the Optimized 24 Constellation, consists of 24 satellites. The orbital parameters for this are provided in Appendix A. These are the positions into which the Block II operational satellites are currently being launched.

In order to account for worst-case conditions, up to three satellite failures were considered in this analysis. A failure is defined to be a satellite which is taken out of service due to operational problems or for maintenance purposes. DoD has guaranteed 21 GPS satellites available 98% of the time [19], although the constellation may perform much better than this.

Satellite failures were selected based on data obtained from analysis that the Aerospace Corporation performed for the GPS Joint Program Office to determine "best", "average", and "worst" case failures. The Aerospace Corp. analysis is based on coverage resulting from setting a PDOP threshold at 6. These satellite failure selections are not optimal for integrity analysis since they were determined for the navigation-only scenario. However, they do provide a baseline for analysis purposes and this eliminates extensive computer simulation which would otherwise be necessary.

The satellite failures used in this study were assumed to be "average" failures from the GPS constellation. From the Aerospace Corp. study, the selections considered to be "average" case failures are: one failure - SV #1, two failures - SVs #4, #23. For the case of three satellite failures, the Optimal 21 Constellation [20] was used since it is assumed that DOD would rephase the satellites to provide optimum coverage if there were only 21 satellites in the GPS constellation. This constellation may provide better availability in some cases than two failures from the GPS constellation since the satellites are optimized for 21 satellites.

8.1.2 Augmentations to the GPS Constellation

RTCA SC-159 has determined that the GPS constellation alone will not satisfy sole means criteria due to the system's low availability for fault detection and isolation. Even a constellation of 24 fully operational satellites can not satisfy the availability requirement since FDI algorithms require a minimum of six visible satellites with good geometry. The results in Table 6 demonstrate this poor performance of stand alone GPS for fault detection and isolation.

Therefore, the system must be augmented in order for it to be considered a sole means navigation system. Several augmentations were examined in this analysis:

1) Use of Barometric Altimeter Aiding
2) Addition of Geostationary Satellites
3) Addition of GLONASS satellites

Other augmentations which are being considered by SC-159 are the use of Loran-C, an inertial system, and the GPS Integrity Channel (GIC). The end goal is to determine which augmentations will satisfy the required navigation performance for a sole means navigation system.

8.1.3 CONUS Grid

An analysis of FDI availability was conducted over the conterminous United States (CONUS) from 50°N to 26°N in latitude and from 125°W to 65°W in longitude. The grid was sampled every 3° in latitude. Each latitude circle has points evenly spaced by 180 nmi in longitude. The analysis was performed over a 24 hour period at five-minute time samples. This grid provides a total of 43,488 space/time samples.

8.1.4 Mask Angle

A satellite mask angle of 7.5° was chosen for this analysis. This is the mask angle which is specified in TSO C129. However, lowering the mask angle can substantially improve availability [21]. RTCA SC-159 has recently proposed reducing the standard 7.5° mask angle to 5°, sighting that 7.5° may be too conservative and is unnecessarily reducing availability. The committee plans to evaluate various mask angles and then make a recommendation. FDI availability results applying lower mask angles will be presented in a follow-on report.

8.1.5 FDI Methods

Most of the FDI availability analysis in this study was performed using the $ARPSUB_{max}$ method. However, as a comparison, the baseline FDE method was also evaluated. The availability of fault detection and isolation was examined for the en route, terminal, and nonprecision approach phases of flight.

As discussed in Section 4, the ARP value is computed for each subset of n-1 visible satellites. The maximum ARP value from these subsets is called $ARPSUB_{max}$. FDI is declared unavailable if the $ARPSUB_{max}$ value for the number of visible satellites exceeds the ceiling value for the phase of flight. The ARP ceiling values are provided in Table 4.

In the FDE method the protection radius is computed for each subset of n-1 visible satellites. The maximum protection radius for these subsets is then compared to the alarm limit for the given phase of flight. These alarm limits are shown in Table 1. If the protection radius exceeds the alarm limit, FDE is said to be unavailable.

8.2 FDI Availability Results

8.2.1 GPS Augmented with Barometric Altimeter Aiding

As mentioned previously, the availability of GPS for FDI without any augmentation was not considered since the FDI availability could not even come close to satisfying the requirements of a sole means system. In fact, even for the use of GPS as a supplemental navigation system, TSO C129 requires the use of barometric altimeter aiding. Therefore, baro aiding of GPS was assumed to be implemented in all of the analyses discussed in this section.

The measurement error standard deviations applied in this analysis for the barometric altimeter are based on TSO C129. These standard deviations are: σ=120 m for en route navigation, σ=300 m for terminal navigation, and σ=50 m for nonprecision approach. The derivation of these values from the TSO is provided in Appendix D.

The results for FDI availability over the CONUS using GPS with baro aiding are shown in Table 9. The availability for en route, terminal, and nonprecision approach was computed using the $ARPSub_{max}$ method.

Table 9 FDI Availability Over CONUS for GPS Augmented with Baro Aiding - $ARPSUB_{max}$ Method

Constellation	En Route	Terminal	NPA
24 SVs - No Failures	98.16%	91.70%	68.30%
24 SVs - 1 Failures	93.85%	86.20%	59.80%
24 SVs - 2 Failures	89.71%	74.67%	46.37%
Optimal 21 Constellation	86.35%	70.47%	37.83%

FDI availability using GPS with baro aiding for en route navigation ranges from approximately 86% with 21 operational satellites to 98% with a fully operational constellation. Although an availability requirement for sole means navigation has not yet been determined, it will most likely be set higher than 99%. Therefore, GPS will undoubtedly require further augmentation in order to satisfy sole means criteria.

In addition to the percentage of availability, it is also important to examine the duration of these outages, as well as the number of occurrences. Figure 7 displays this information for the en route phase of flight. It should be noted that the number of outage occurrences, plotted on the y-axis, is on a logarithmic scale. The number of outages is found by subtracting the value at the lower boundary of the shaded area from the value at the upper boundary. For example, the number of five-minute outages for the GPS 24 with one failure case is approximately (550 - 210) = 340.

With a constellation of 24 operational satellites, outages at a specific location can last up to 40 minutes. The longest outage experienced for en route navigation was 80 minutes. The reason

that the one satellite failure case has an outage which lasts slightly longer than outages for the 22 and 21 satellite constellations is due to the choice of satellite failures. As discussed previously, the failure selections are not ideal for integrity analysis since they are based on navigation criteria. Therefore, a satellite failure which is deemed to be "average" for navigation could turn out to be a "worst" case selection for integrity analysis.

As shown in Figure 7, the number of outage occurrences decreases as the length of the outages increases. This is a characteristic of GPS for all phases of flight and results from the changing geometry of the satellites.

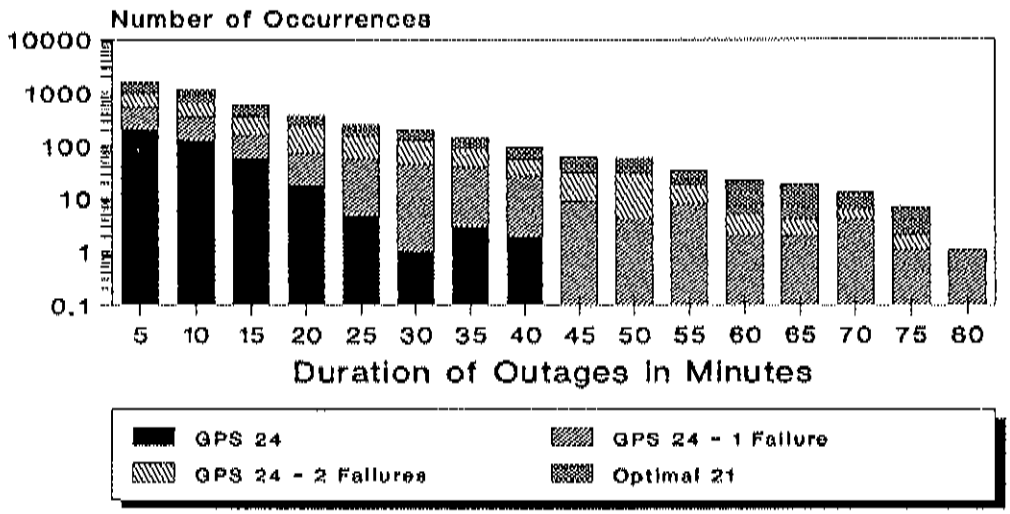

Figure 7 Duration of Outages Over CONUS for En Route Navigation - GPS Augmented with Baro Aiding

For terminal navigation, FDI is available almost 92% of the time with 24 operational satellites and baro aiding. Having one failure drops the availability to 86.2%, two satellite failures to 74.7%, and using the Optimal 21 Constellation FDI is available approximately 70.5% of the time. With a standard deviation of 300 m, the baro altimeter does not provide as much aiding for terminal navigation as it does during other phases of flight. The reason for the higher error is that it is more difficult to calibrate the altimeter as the aircraft descends through different altitudes in the terminal phase of flight.

The outage duration and number of occurrences for terminal navigation are presented in Figure 8. Outages last up to 70 minutes for the case of 24 operational satellites. The maximum outage duration is approximately three hours and occurs for the case of two failures from constellation. Again, the 21 satellite constellation has a shorter outage duration than the 22 satellite case because these satellite locations have been optimized for the best coverage.

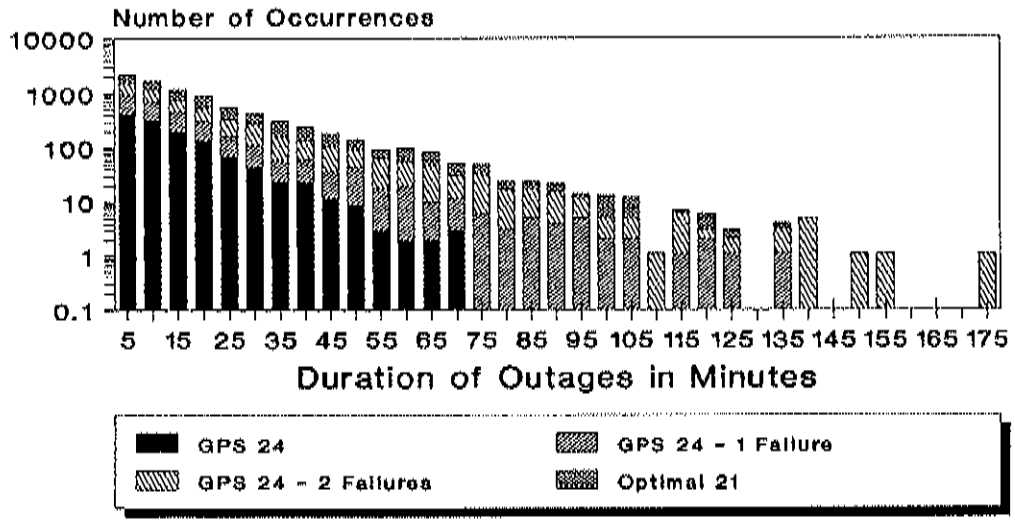

Figure 8 Duration of Outages Over CONUS for Terminal Navigation - GPS Augmented with Baro Aiding

As shown in Table 9, the availability of GPS with baro aiding to perform fault detection and isolation during non precision approach is very low. Even with 24 operational satellites, FDI availability is less than 70% and with only 21 satellites operating it is available only about 38% of the time.

Figure 9 displays the duration of outages vs. the number of occurrences for NPA navigation. With such poor availability, the length of the outages is quite long. In the case of 24 GPS satellites, outages last over two hours. Outages can last up to five hours when two failures in the constellation occur.

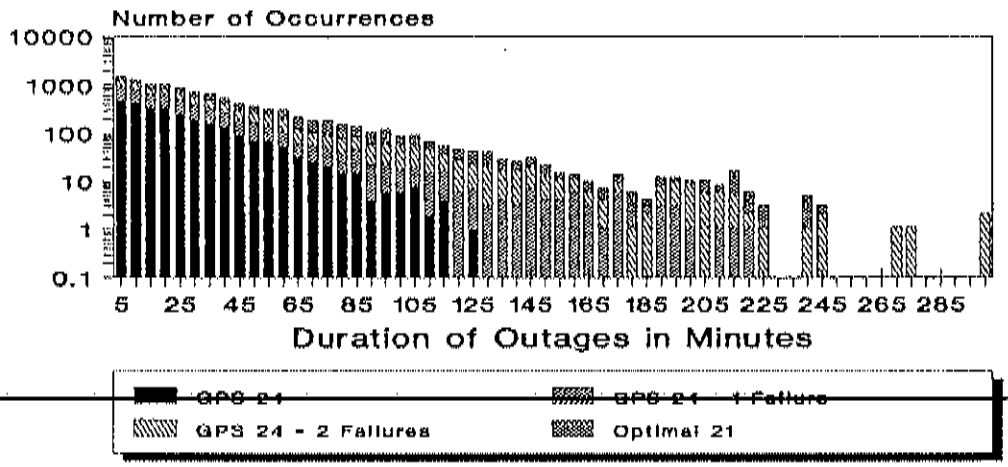

Figure 9 Duration of Outages Over CONUS for NPA Navigation - GPS Augmented with Baro Aiding

A similar analysis using the baseline FDE method for GPS with baro aiding was performed in order to compare the performance of the two algorithms. The results for FDE, presented in Table 10, are similar to those shown in Table 9 for the $ARPSUB_{max}$ method. FDI vs. FDE availability for en route navigation differs by less than one percent. For terminal navigation, availability using the $ARPSUB_{max}$ method is approximately one percent higher than that of the FDE method. The biggest difference between the two algorithms appears in the nonprecision approach case. For all four constellations, the availability applying the FDE method is approximately 4% lower than that obtained for FDI using the $ARPSUB_{max}$ method.

Table 10 FDI Availability Over CONUS for GPS Augmented with Baro Aiding - FDE Method

Constellation	En Route	Terminal	NPA
24 SVs - No Failures	98.07%	91.02%	64.76%
24 SVs - 1 Failure	93.62%	85.17%	55.97%
24 SVs - 2 Failures	89.30%	73.40%	43.13%
Optimal 21 Constellation	85.85%	68.70%	34.80%

For en route and terminal navigation, both the FDE and FDI ($ARPSub_{max}$) methods have the same maximum outage duration for RAIM. However, there are more occurrences of outages using the FDE method than there are for the $ARPSub_{max}$ algorithm. During NPA, the maximum outage for the FDE method is an hour longer than that for the $ARPSub_{max}$ algorithm. As in the previous two phases of flight, there are also more occurrences of outages for the FDE method.

8.2.2 GPS Constellation Augmented with Three Geostationary Satellites

GPS augmented with ranging geostationary satellites covering the CONUS greatly enhances the availability of FDI for all constellations considered in this analysis. The Wide Area GPS Augmentation (WGA) will be designed such that the user can range on the geostationary satellites, as well as receive integrity information from them. The geostationary satellites will broadcast a GPS-like signal at L-band. Studies show that RAIM (FDI) and GIC are complementary methods for providing GPS integrity information and should work together [22].

Three ranging geostationary satellites which provide coverage over the CONUS were used in this analysis. They were assumed to be at the following INMARSAT locations with corresponding longitudes: Atlantic Ocean Region West (AORW) 55.5° W, Atlantic Ocean Region East (AORE) 18.5° W, and Pacific Ocean Region (POR) 180°. Using these satellite positions, both the eastern and western portions of the CONUS receive dual geostationary coverage. The middle of the country has only the AORW satellite in view. FDI availability over CONUS is shown in Table 11 using GPS augmented by three geostationary satellites and baro aiding.

Table 11 FDI Availability Over CONUS for GPS Augmented with Three Geostationary SVs and Baro Aiding

Constellation	En Route	Terminal	NPA
24 SVs - No Failures	99.99%	99.53%	95.24%
24 SVs - 1 Failure	99.77%	97.88%	90.61%
24 SVs - 2 Failures	99.81%	97.42%	85.77%
Optimal 21 Constellation	99.60%	96.39%	86.42%

For en route navigation, FDI is available well over 99% of the time, even when only 21 satellites are operational. The reason that the one satellite failure case provides a little bit lower availability than the case of two failures is again the choice of satellite failures. However, for the terminal and nonprecision approach phases of flight, the two satellite failure scenario has a lower availability than that provided with only one satellite failure.

An explanation for this occurrence is that when SV #1 is removed from the constellation, there are space/time points where the ARP value is very high and exceeds the ceiling value for all three phases of flight. When SVs #4 and #23 are removed from the constellation the overall geometry is worse than having only one satellite failed. However, there are some ARP values which exceed the terminal and NPA ceiling values, but are within the en route protection limit. Therefore, the two satellite failure constellation has a lower availability during terminal and NPA navigation than the constellation having one satellite failure, but for en route navigation the situation is reversed.

The duration of outages and number of occurrences for en route navigation are displayed in Figure 10. The GPS constellation with 24 operational satellites when augmented by geostationary satellites and baro aiding experiences only three occurrences of five minute outages. The maximum outage duration for the scenarios evaluated is 40 minutes, which occurs when SV #1 is removed from the constellation. Figure 10 demonstrates that in addition to shorter outage durations, the number of occurrences is significantly reduced.

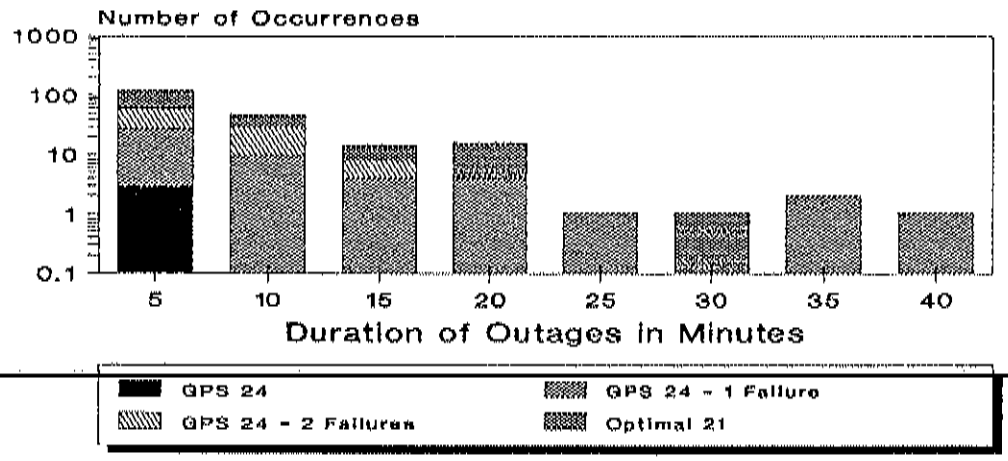

Figure 10 Duration of Outages Over CONUS for En Route Navigation - GPS Augmented with 3 Geos and Baro Aiding

FDI availability for terminal navigation is greater than 99% for a GPS constellation of 24 satellites when augmented with 3 geostationary satellites and baro aiding. Availability ranges from approximately 96% to 98% for the other constellations evaluated in this analysis.

As shown in Figure 11, outages can last up to an hour with 24 operational satellites, 3 geos, and baro aiding. However, the number of occurrences for each outage duration is still fairly low. The longest outage duration at a specific location for terminal navigation is 85 minutes.

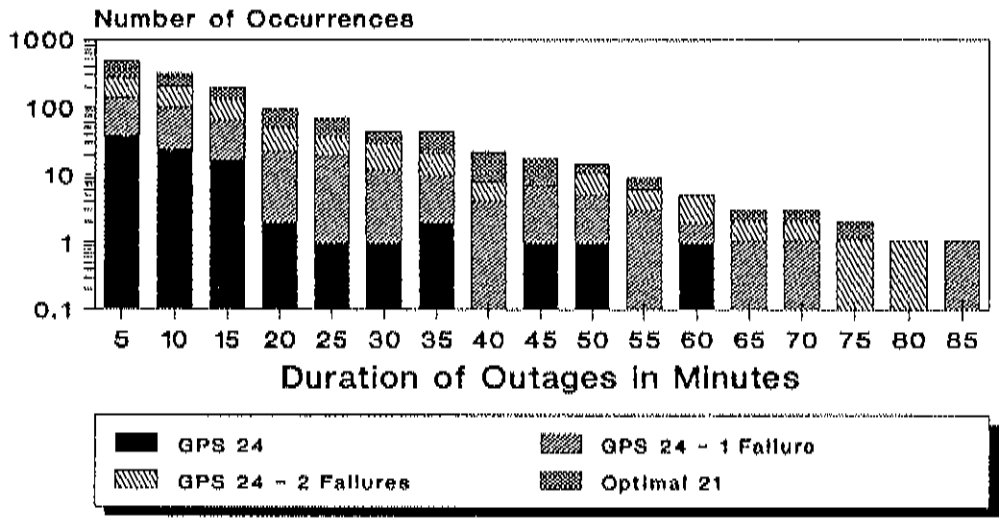

Figure 11 Duration of Outages Over CONUS for Terminal Navigation - GPS Augmented with 3 Geos and Baro Aiding

The benefit of adding geostationary satellites to increase FDI availability is most clearly demonstrated for the case of nonprecision approach navigation. Although the availability is still lower than that required for a sole means system, it is significantly increased compared to that achieved not using the geos (See Table 9). For instance, in the Optimal 21 Constellation the availability of FDI more than doubles.

Figure 12 presents the outage durations and number of occurrences for nonprecision approach navigation. As expected, outages last much longer than those for the en route and terminal phases of flight. In the case of two failures from the constellation, the outage duration is almost 2.5 hours. However, this is a 50% reduction from the maximum outage duration for NPA without the aiding of geostationary satellites.

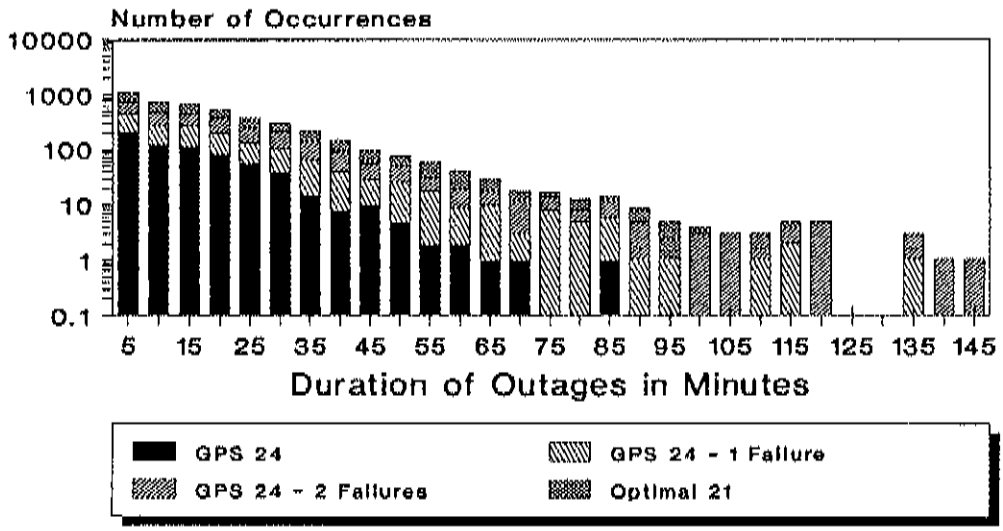

Figure 12 Duration of Outages Over CONUS for NPA Navigation - GPS Augmented with 3 Geos and Baro Aiding

8.2.3 GPS Constellation Augmented with GLONASS

GLONASS is a satellite radionavigation system which is currently being deployed by the Commonwealth of Independent States (CIS). Similar to GPS, the GLONASS constellation is also planned to consist of 24 satellites. However, there is some question as to whether or not the CIS can financially maintain a 24 satellite constellation. GLONASS satellites orbit in three planes of eight satellites each at an inclination angle of 64.8°, and at a slightly lower altitude than GPS.

Several other differences exist between the two constellations. There is no plan to include Selective Availability on the GLONASS satellites. Each GLONASS satellite is assigned to a separate frequency, whereas GPS satellites are all on the same frequency. Differences also exist in the coordinate reference frame: GLONASS is referenced to the Soviet Geodetic System of 1990 (SGS 90), while GPS is referenced the World Geodetic System of 1984 (WGS 84). Also, for timing GLONASS is referenced to Soviet Union Universal Coordinated Time (UTC SU) and GPS is referenced to the U.S. Naval Observatory Universal Coordinated Time (UTC USNO).

The orbital parameters for the GLONASS constellation used in this study are provided in [23]. Unfortunately, the full benefit of adding more satellites to the GPS constellation is not obtained since some of the GLONASS satellites are located near GPS satellites. Therefore, there are cases when the geometry of visible satellites is not significantly improved.

In this analysis, GPS was augmented with one, two, and three planes of GLONASS satellites. The CIS is currently launching satellites into the first and third planes of their constellation. There have been no satellites launched into the second plane. For the case of using only one plane of GLONASS to augment GPS, the first plane was chosen. Planes one and three were chosen for the two plane augmentation. Again, the use of the barometric altimeter was also implemented.

The results of GPS augmented with GLONASS and baro aiding are provided in Table 12. The only augmentation of those analyzed in this study which provides 100% availability for all three phases of flight is a 24 satellite GPS constellation augmented with the full three planes of GLONASS and baro aiding.

Table 12 FDI Availability Over CONUS for GPS Augmented with GLONASS and Baro Aiding

Constellation	En Route	Terminal	NPA
24 SVs + 1 Plane GLONASS	99.82%	98.82%	94.02%
21 SVs + 1 Plane GLONASS	98.63%	96.11%	82.68%
24 SVs + 2 Planes GLONASS	100%	100%	99.68%
21 SVs + 2 Planes GLONASS	100%	99.96%	96.59%
24 SVs + 3 Planes GLONASS	100%	100%	100%
21 SVs + 3 Planes GLONASS	100%	100%	99.98%

For en route navigation, FDI is available 100% of the time when augmented by two or more planes of GLONASS satellites. Figure 13 displays the duration of outages vs. the number of occurrences when GPS is augmented with one plane of GLONASS satellites. With 24 GPS satellites, outages last up to 40 minutes and with 21 GPS satellites outages can last up to an hour. As shown in the figure, the number of outage occurrences is very low, especially when there are 24 operational GPS satellites.

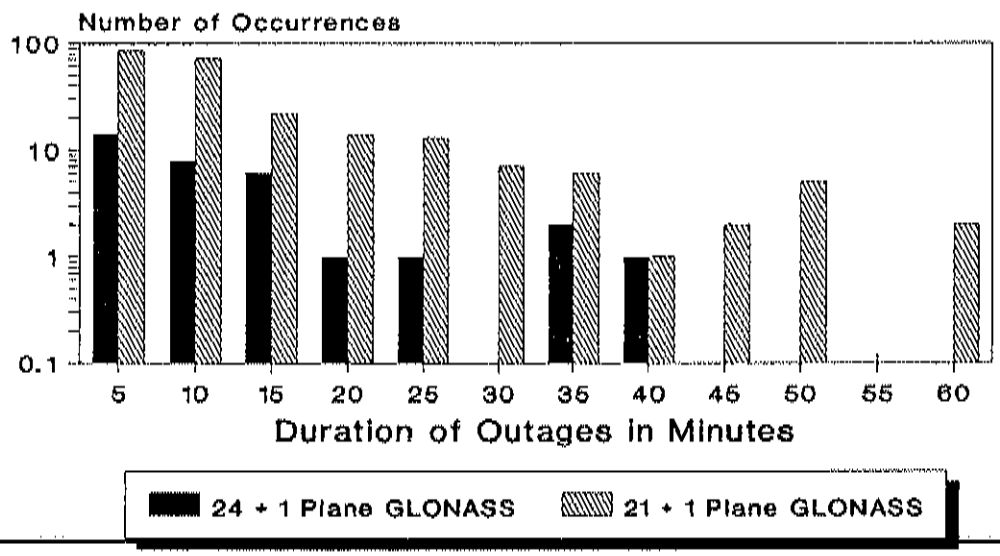

Figure 13 Duration of Outages Over CONUS for En Route Navigation - GPS Augmented with GLONASS and Baro Aiding

In the terminal navigation phase of flight, 100% availability can again achieved for the following cases: 24 GPS satellites augmented with two or more planes of GLONASS satellites or 21 GPS satellites augmented with three planes of GLONASS satellites.

The outage durations vs. number of occurrences are presented in Figure 14. Outages last up to 65 minutes for 24 GPS satellites and up to 70 minutes for 21 GPS satellites, each augmented with one plane of GLONASS and baro aiding. With 21 GPS satellites and two planes of GLONASS with baro aiding, outages are restricted to a maximum of 20 minutes.

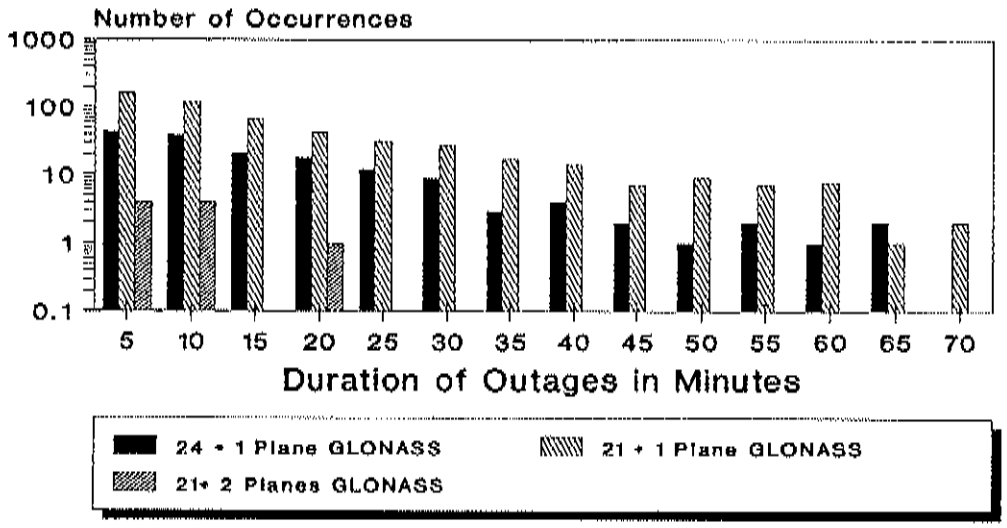

Figure 14 Duration of Outages Over CONUS for Terminal Navigation - GPS Augmented with GLONASS and Baro Aiding

During nonprecision approach navigation, the only combination of satellites to provide 100% FDI availability is 24 GPS satellites plus the full three planes of GLONASS satellites and baro aiding.

As shown in Figure 15, the outages are quite long for nonprecision approach when GPS is only augmented with one plane of GLONASS and the baro altimeter. Outages last over an hour for 24 GPS satellites and up to 3.5 hours with only 21 GPS satellites. In the case of 24 GPS and 24 GLONASS satellites, there are no outages and with 21 GPS satellites and all of the GLONASS satellites operational, outages are restricted to a maximum of five minutes.

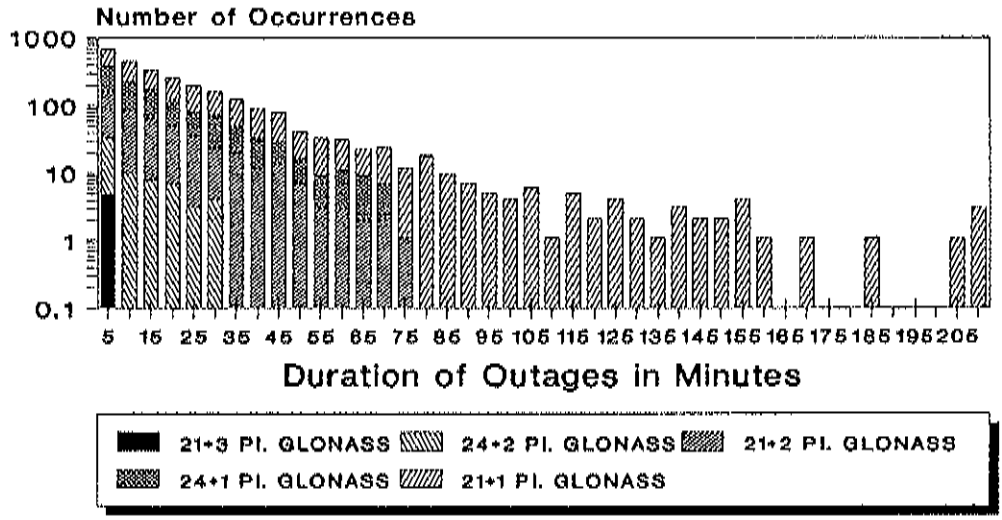

Figure 15 Duration of Outages Over CONUS for NPA Navigation - GPS Augmented with GLONASS and Baro Aiding

9. SUMMARY AND CONCLUSIONS

This study provides a detailed mathematical description of GPS fault detection and isolation using the ARP RAIM method. The differences between the ARP FDI algorithm and the RTCA baseline fault detection and exclusion algorithm are discussed.

Dynamic testing of the two algorithms was performed by introducing a ramp-type bias error into each of the two most-difficult-to-isolate satellites. The initial testing was performed for nonprecision approach using satellite geometries with seven satellites in view. The results indicate that there is not a great difference in the performance of the FDI and FDE algorithms for the seven-in-view case. Both methods appear to come close to satisfying the RTCA miss probability specifications. Minor modifications may be needed in the geometry screening criteria in order to meet the specified .001 miss rate.

The comparison of the FDI and FDE algorithms for nonprecision approach will continue by examining satellite geometries with eight and nine visible satellites. A similar comparison also will be performed for terminal and en route navigation.

This study also provided an analysis of FDI availability over CONUS for GPS with augmentations of a barometric altimeter, geostationary satellites, and GLONASS satellites. Availability was analyzed for the en route, terminal, and nonprecision approach phases of flight. The availability of FDI, as well as FDE, was evaluated for the GPS plus baro aiding case. FDI provided slightly better availability than the FDE algorithm. The results demonstrate that GPS augmented only with a baro altimeter does not have a high availability, especially for the nonprecision approach phase of flight. The availability substantially increases with the augmentation of GLONASS and geostationary satellites. However, the only scenario analyzed in this study which provided 100% availability for all three phases of flight was 24 GPS satellites with 24 GLONASS satellites and baro aiding.

Future analysis will examine the availability of FDI when lower mask angles are applied. FDI availability will also be analyzed using ranging signals from geostationary satellites in the Defense Satellite Communication System (DSCS). Efforts will continue in order to determine the minimum number of satellites needed to satisfy availability requirements for sole means navigation.

Finally, a new Partial-Identification RAIM (PIR) algorithm will be investigated. The PIR algorithm attempts to capitalize on the best features of the FDI and FDE algorithms. This method is characterized by observing all visible satellites until a detection occurs and then excluding the two satellites most likely to have failed. This algorithm has the potential to improve availability significantly.

10. REFERENCES

[1] *Minimum Operational Performance Standards for Airborne Supplemental Navigation Equipment Using Global Positioning System (GPS)*, Document No. RTCA/DO-208, July 1991, Prepared by: SC-159.

[2] R.G. Brown, G.Y. Chin, and J.H. Kraemer, *RAIM: Will It Meet the RTCA GPS Minimum Operational Performance Standards?* Proceedings of the National Technical Meeting of The Institute of Navigation, Phoenix, AZ, January 22-24, 1991, pp. 103-111.

[3] R.G. Brown, G.Y. Chin, and J.H. Kraemer, *Update on GPS Integrity Requirements of the RTCA MOPS*, Proceedings of the Fourth International Technical Meeting of the Satellite Division of The Institute of Navigation (ION GPS-91), Albuquerque, NM, September 11-13, 1991, pp. 761-772.

[4] G.Y. Chin, and J.H. Kraemer, *GPS Integrity Simulation Using Approximate Radial-Error Protected (ARP) Criterion*, Project Memorandum DOT-VNTSC-FA160-PM-91-3, September 1991, RSPA/Volpe National Transportation Systems Center, Cambridge, MA.

[5] G.Y. Chin, and J.H. Kraemer, *Screening Out Bad Geometries in GPS Using Approximate Radial-Error Protected (ARP) Criterion*, Project Memorandum DOT-VNTSC-FA260-PM-92-11, September 1992, RSPA/Volpe National Transportation Systems Center, Cambridge, MA.

[6] G.Y. Chin, J.H. Kraemer, and R. G. Brown, *GPS RAIM: Screening Out Bad Geometries Under Worst-Case Bias Conditions*, NAVIGATION: Journal of The Institute of Navigation, Vol. 39, No. 4, Winter 1992-93, pp. 407-427.

[7] M.A. Sturza, *Navigation System Integrity Monitoring Using Redundant Measurements*, NAVIGATION, Journal of The Institute of Navigation, Vol. 35, No. 4, Winter 1988-89, pp. 483-501.

[8] M.A. Sturza and A.K. Brown, *Comparison of Fixed and Variable Threshold RAIM Algorithms*, Proceedings of the Third International Technical Meeting of the Satellite Division of The Institute of Navigation (ION GPS-90), September 19-21, 1990, Colorado Springs, CO, pp. 437-443.

[9] B.W. Parkinson and P. Axelrad, *A Basis for the Development of Operational Algorithms for Simplified GPS Integrity Checking*, Proceedings of The Institute of Navigation Satellite Division First Technical Meeting, Colorado Springs, September 1987, pp. 269-276.

[10] B.W. Parkinson and P. Axelrad, *Autonomous GPS Integrity Monitoring Using the Pseudorange Residual*, NAVIGATION: Journal of The Institute of Navigation, Vol. 35, No. 2, Summer 1988, pp. 255-274.

[11] B.W. Parkinson and P. Axelrad, *A Practical Algorithm for Autonomous Integrity Verification Using the Pseudo Range Residual*, Proceedings of The Institute of Navigation National Technical Meeting, Santa Barbara, CA, 1988, pp. 254-260.

[12] B.W. Parkinson and P. Axelrad, *Receiver Autonomous Integrity Monitoring of the Navigation Service Provided by the Global Positioning System*, Report prepared for the Department of Transportation, Research and Special Programs Administration, Transportation System Center, Cambridge MA, May 1989; Contract No. 88-P-82289.

[13] N.L. Johnson and S. Kotz, *Noncentral χ^2 Distribution*, In: Distributions in Statistics: Continuous Univariate Distributions-2, Chapt. 28, Houghton Mifflin Co., 1970.

[14] R.G. Brown and P.Y.C. Hwang, Introduction to Random Signal Analysis and Applied Kalman Filtering (2nd Ed.), Wiley, 1992.

[15] R.G. Brown, *A Baseline RAIM Scheme and a Note on the Equivalence of Three RAIM Methods*, Proceedings of the National Technical Meeting of The Institute of Navigation, San Diego, CA, January 27-29, 1992, pp. 127-137.

[16] Memorandum from John Studenny to Larry Chesto, RTCA Paper No.148-93/SC159-424, March 17, 1993.

[17] R.G. Brown, Private communication to J.H. Kraemer.

[18] Federal Aviation Administration, Aircraft Certification Service, *Technical Standard Order TSO C129*, December 10, 1992.

[19] Federal Radionavigation Plan, DOT-VNTSC-RSPA-92-2/DOD-4650.5, January 1993.

[20] Green, G.B., Massatt, P.D., Rhodus, N.W., *The GPS 21 Primary Constellation*, NAVIGATION, Journal of The Institute of Navigation, Vol. 36, No. 1, Spring 1989, pp. 9-24.

[21] Van Dyke, Karen L., *Analysis of Worldwide RAIM Availability for Supplemental Navigation*, Project Memorandum DOT-VNTSC-FA360-PM-93-4, May 1993.

[22] Brown, R. Grover, *RAIM and GIC Working Together: The Ultimate Solution to the GPS Integrity Problem*, NAVIGATION, Journal of The Institute of Navigation, Vol. 36, No. 2, Summer 1989, pp. 173-178.

[23] Daly, P., Lennen, G.R., *GLONASS C/A Code Signals - Status & Developments*, Proceedings of the Second International Technical Meeting of the Satellite Division of The Institute of Navigation (ION GPS-89), Colorado Springs, Co, September 27-29, 1989, pp. 53-60.

APPENDIX A. TARGET LOCATIONS FOR OPTIMIZED 24 CONSTELLATION

(From the Summary Record of the Civil GPS Service Interface Committee Meeting, January 30, 1992.)

The following parameters describe the target location orbital elements of the Optimized 24 GPS Constellation.

	Orbital Plane	Semimajor Axis	Eccentricity	Inclination Angle	Rt. Ascension Ascending Node	Arg. of Perigee	Mean Anomaly
1.	A1	26559800.	0.0	55.0	296.23	0.0	265.92
2.	A2	26559800.	0.0	55.0	295.33	0.0	96.05
3.	A3	26559800.	0.0	55.0	296.23	0.0	56.03
4.	A4	26559800.	0.0	55.0	296.23	0.0	162.37
5.	B1	26559800.	0.0	55.0	361.23	0.0	335.20
6.	B2	26559800.	0.0	55.0	354.57	0.0	67.58
7.	B3	26559800.	0.0	55.0	356.23	0.0	98.62
8.	B4	26559800.	0.0	55.0	354.33	0.0	204.22
9.	C1	26559800.	0.0	55.0	56.23	0.0	6.12
10.	C2	26559800.	0.0	55.0	56.23	0.0	135.80
11.	C3	26559800.	0.0	55.0	56.23	0.0	233.91
12.	C4	26559800.	0.0	55.0	56.23	0.0	266.04
13.	D1	26559800.	0.0	55.0	116.23	0.0	29.47
14.	D2	26559800.	0.0	55.0	116.23	0.0	61.60
15.	D3	26559800.	0.0	55.0	117.52	0.0	159.69
16.	D4	26559800.	0.0	55.0	119.36	0.0	289.40
17.	E1	26559800.	0.0	55.0	176.59	0.0	91.29
18.	E2	26559800.	0.0	55.0	175.20	0.0	196.84
19.	E3	26559800.	0.0	55.0	176.89	0.0	227.93
20.	E4	26559800.	0.0	55.0	177.36	0.0	320.31
21.	F1	26559800.	0.0	55.0	236.23	0.0	133.13
22.	F2	26559800.	0.0	55.0	236.23	0.0	239.47
23.	F3	26559800.	0.0	55.0	234.46	0.0	359.45
24.	F4	26559800.	0.0	55.0	236.23	0.0	29.59

~~The epoch date for this constellation is midnight Dec. 1, 1991 (1991,12,1,0,0,0).~~

APPENDIX B. CHI-SQUARE DENSITY FUNCTIONS OF SPECIAL INTEREST

The general formula for the chi-square density functions is provided in Section 3. The functions given here allow one to compute the detection thresholds for various numbers of degrees of freedom.

n = 1: (n = chi-square degrees of freedom)

$$f_x(x) = \frac{1}{\sqrt{2\pi}} x^{-\frac{1}{2}} e^{-\frac{x}{2}} \qquad \text{(Mean = 1)}$$

(One can use normal density tables for this function by working with |R.V.|, and noting $|R.V.| = \sqrt{(R.V.)^2}$)

n = 2:

$$f_x(x) = \frac{1}{2} e^{-\frac{x}{2}} \qquad \text{(Mean = 2)}$$

(This function can be integrated explicitly.)

n = 3:

$$f_x(x) = \frac{1}{\sqrt{2\pi}} x^{\frac{1}{2}} e^{-\frac{x}{2}} \qquad \text{(Mean = 3)}$$

(This function is difficult to integrate without extensive tables. The detection threshold can be determined by interpolating the results of n=2 and n=4 to get the result for n = 3.)

n = 4:

$$f_x(x) = \frac{1}{4} x e^{-\frac{x}{2}} \qquad \text{(Mean = 4)}$$

(This function can be integrated by parts, or may be found in tables of integrals.)

n = 5:

$$f_x(x) = \frac{1}{3\sqrt{2\pi}} x^{\frac{3}{2}} e^{-\frac{x}{2}} \qquad \text{(Mean = 5)}$$

(This function is difficult to integrate without extensive tables. The detection threshold can be extrapolated from the n = 3 and n = 4 cases to get the result for n = 5.)

APPENDIX C. FACTOR $\sqrt{(n-4)}$ IN RELATIONSHIPS BETWEEN VARIABLES IN EARLIER STUDIES AND THE PRESENT STUDY

Let F denote $\sqrt{(n-4)}$.

Let the symbol {1} be used to mark the quantities of interest in the present study and {2} be used to mark those of previous studies [3-6,15] by the present authors. In the present study, one has the following:

(10a) Test Statistic(j,b){1} (no-noise) $= \sqrt{SSE(j)}$

(10b) $= b\sqrt{(1-B_{jj})}$

One also has the No-Noise Horizontal Radial Error:

(11) $R_{hj}(b) = b\sqrt{(A_{1j}^2 + A_{2j}^2)}$

The expression for $R_{hj}(b)$ is the same as used in previous studies.

(12) SLOPE {1} ≡ (Horiz. Nav. Radial Error)/(Test Statistic {1})

(13) $SLOPE(j)\{1\} = \sqrt{\frac{(A_{1j}^2 + A_{2j}^2)}{(1-B_{jj})}}$

One finds the following:

Test Statistic(j,b){2} (no-noise) = Test Statistic(j,b){1}/F

It follows from the above equation that

Threshold{2} = Threshold{1}/F

SLOPE(j){2} = SLOPE(j){1}F

Now

(14) ARP{2} (meters) = $SLOPE_{max}\{2\}$ (dimensionless) × Detection Threshold{2} (meters)

$$= \text{SLOPE}_{max}\{1\}F \times \text{Detection Threshold}\{1\}/F$$

$$= \text{SLOPE}_{max}\{1\} \times \text{Detection Threshold}\{1\}$$

$$= \text{ARP}\{1\}$$

One sees that the expression for ARP and $R_{hj}(b)$ are unchanged.

APPENDIX D JUSTIFICATION OF THE σ_{baro} VALUES USED IN THE RTCA FDI ANALYSIS

1. Nonprecision Approach

σ_{baro} for this phase of flight is assumed to be 50m. This value is designated as an "acceptable" assumption on page 13 of [18].

2. En route

σ_{baro} for en route is assumed to be 120m. This was obtained by using the equation at the top of page 24 of [18]. The equation is:

σ_{baro} = RSS Combination of e_v, $b_{el} * v * t$, and b_{en}

The scenario assumed here is that the barometric altimeter measurement is continuously calibrated by GPS up to a span of time where there would be a RAIM outage without the altimeter measurement. An average outage span of 15 min. is assumed. The components of σ_{baro} are computed as follows:

$e_v = (VDOP_{max}) * \sigma_{sv} = (3) * (33.3) = 100m$

b_{en} = (13m/1000' altitude change)*(2) = 26m
(2000' altitude change in 15min was assumed.)

$b_{el} * v * t$ = (0.5m/nmi) * (500knots) * (15min)
= 62.5m

RSS Total = $\sqrt{(100)^2 + (26)^2 + (62.5)^2}$ = 120.7m

This was rounded to 120m in the availability study.

3. Terminal

This is the most difficult σ_{baro} to compute, because it depends so much on the assumed flight scenario. GPS barometric altimeter calibration is assumed just prior to a descent from high altitude. At the beginning of the descent, a RAIM outage (without benefit of barometric altimeter augmentation) is assumed. A descent from 30,000 to 6,000 ft. was calculated as follows (see page 24 of [18]):

a) First 12,000 ft:
(13m/1000')*(12) = 156m

b) Next 12,000 ft:
(23m/1000')*(12) = 276m

Total b_{en} = 432m

The calibration error is same as for the en route phase. Therefore,

e_u = 100m

The (b_{el} * v * t) term is assumed to be negligible relative to the b_{en} term. Therefore,

RSS Total = $\sqrt{(423)^2 + (100)^2}$ = 443.4m

However, this is an extreme situation, because it represents the error at the end of the descent. Averaging the initial and final rms errors yields:

Ave. rms error = (443 + 100) / 2 ≈ 272m

This figure was then "rounded up" about 10% to account for some descent below 6,000 ft., which could occur in terminal flight. The final σ_{bnro} used was then 300m.

Note. The σ-values of 50, 120, and 300m were used for availability analysis purposes only. It should be recognized that more refined values could be computed and used online if this is deemed necessary.